

# TOPOLOGICAL VORTEX IDENTIFICATION FOR HAMILTONIAN FLOWS IN DOUBLY PERIODIC DOMAINS

MITSUAKI KIMURA, TAKASHI SAKAJO, AND TOMOO YOKOYAMA

ABSTRACT. The motion of two-dimensional incompressible and viscous fluids in doubly periodic domains is often used as a numerical model to investigate the dynamics and statistical properties of two-dimensional (2d) turbulence. In the study of 2d turbulence, it is important to describe interactions of coherent vortex structures of various sizes in turbulent flows, but identifying such vortex structures accurately from complex flow patterns is not easy. In this paper, we provide a classification theory for the topological structure of particle orbits generated by two-dimensional Hamiltonian flows on a flat torus  $\mathbb{T}^2$ , which is a mathematical model of 2d incompressible and viscous flows. Based on this theory, we show that the global orbit structure of every Hamiltonian flow is converted into a planar tree, called a *partially Cyclically-Ordered rooted Tree (COT)*, and its string expression (COT representation). Applying the conversion algorithm to snapshots of two-dimensional free-decaying turbulence and enstrophy cascade turbulence, we demonstrate that the topological structure of a complex flow pattern can be represented by a simple tree and a sequence of letters by the conversion algorithm, thereby extracting coherent vortex structures successfully from the viewpoint of topology.

## 1. INTRODUCTION

We consider the flow generated by an inviscid and incompressible fluid of a constant density on a flat torus  $\mathbb{T}^2$ , i.e., a two-dimensional domain with a doubly periodic boundary condition. The evolution of the velocity field  $\mathbf{u}(\mathbf{x}, t) = (u(x, y, t), v(x, y, t))$  at  $\mathbf{x} = (x, y) \in \mathbb{T}^2$  and time  $t \in \mathbb{R}$  is governed by the Navier-Stokes equation.

$$\partial_t \mathbf{u} + (\mathbf{u} \cdot \nabla) \mathbf{u} = -\nabla p + \nu \Delta \mathbf{u} + \mathbf{f}, \quad \nabla \cdot \mathbf{u} = 0,$$

in which  $p(\mathbf{x}, t)$  and  $\mathbf{f}$  denote the pressure and the external force. For a smooth velocity field, we define the stream function  $\psi(\mathbf{x}, t)$  by  $(u, v) = (\partial_y \psi, -\partial_x \psi)$  and the vorticity  $\omega(\mathbf{x}, t) = \partial_x v - \partial_y u$  respectively, the Navier-Stokes equation is reduced to

$$\partial_t \omega + \mathcal{J}(\omega, \psi) = \nu \Delta \omega + \tilde{\mathbf{f}}, \quad -\Delta \psi = \omega,$$

where  $\mathcal{J}(f, g)$  represents the Jacobi matrix for functions  $(f, g)$ , and a scalar function  $\tilde{\mathbf{f}}$  is defined by  $\nabla \times \mathbf{f} = (0, 0, \tilde{\mathbf{f}})$ .

These fluid equations on a flat torus are commonly used to investigate two-dimensional turbulent flows numerically to clarify the relation between its statistical properties and complex flow structures, since accurate schemes such as the spectral

---

*Date:* October 29, 2024.

*Key words and phrases.* Topological flow data analysis, Hamilton flows, doubly periodic, 2D turbulence, vortex identification.

T. S. is partially supported by JST MIRAI JPMJMI22G1.

method are available. See a comprehensive survey paper by Tabeling [12] for the physics of two-dimensional turbulence. Typically, two types of two-dimensional turbulence are studied. One is called free decaying turbulence. It describes how a complex flow relaxes into a simpler flow pattern under no external force  $\tilde{f} = 0$  while losing its energy due to viscous dissipation. The other is known as inverse cascade turbulence. When a large-scale external force is applied to a flow, we investigate the ensemble average of the energy spectra, which is the  $L^2$  norm of the velocity field, and the enstrophy spectra, which is the  $L^2$  norm of vorticity. We also observe that the complex flow pattern with many coherent vortex structures gradually transitions to that with larger-scale vortices. The decaying process is characteristic of two-dimensional turbulence, and it is often investigated as the interactions among coherent vortex structures of various scales in complex turbulent flow patterns. Hence, extracting coherent vortex structures from complex flow patterns is an essential task in the study of two-dimensional turbulence.

Various methods have been proposed to extract the coherent rotational component from the vorticity distribution. For instance, McWilliams [8] proposed an intuitive method of finding the point where the vorticity is at its extreme value and extracting a closed contour enclosing the vorticity region around the point. Basdevant [1] and Hua & Klein [5] defined a rotational flow component using the eigenvalues of the velocity gradient tensor based on the Weiss assumption that it varies very slowly. Farge [3] used the wavelet transform of the vorticity and coherent rotating regions which have been extracted corresponding to the coefficients of an appropriate scale. All of these methods extract coherent vortex structures from the vorticity function. On the other hand, since vorticity has large values not only in rotating flow regions but also in strong shear regions, it is still unclear how we define a vortex region. Hence, it is inevitable to introduce certain empirical hyperparameters and working hypotheses for vortex identifications in these methods.

As an alternative approach to extracting coherent rotating flow structures from two-dimensional flow patterns, a method called Topological Flow Data Analysis (TFDA) has been developed based on topology and the theory of dynamical systems. Let us recall that the flow field constructed here is a Hamiltonian vector flow with the stream function  $\psi$  being its Hamiltonian function. Then, the particle orbits (streamlines) generated by an instantaneous Hamiltonian vector field coincide with the level curves of the Hamiltonian function owing to  $\nabla\psi \cdot \mathbf{u} = 0$ . Therefore, a topological classification of Hamiltonian flows is nothing but a classification of the topological structure of the level curves. Ma and Wang [7] considered such a Hamiltonian vector field on  $\mathbb{R}^2$ . They show that the topological structures of particle orbits consist of a finite number of topologically distinguishable local flow patterns under the condition of structural stability in  $C^r$  ( $r \geq 1$ ) topology. In [16], it is shown that this topological classification theory can be extended to Hamiltonian flows in the presence of uniform flows, and that the global topological structures of the Hamiltonian flows are expressed as a sequence of letters arranged according to a certain rule. Later, it is discovered that the global topological structure is converted into a planar tree uniquely [9], which is now called a partially cyclically-ordered rooted tree (COT), and its symbolic representation is named COT representation [15]. It is found that COT is isomorphic to the Reeb graph of Hamiltonian functions as abstract graph [14]. Consequently, TFDA allows

us to distinguish the topological structures of flow patterns with COT and COT representation.

Furthermore, using this COT, we can extract the area surrounded by a self-connected saddle separatrix as a coherent rotational flow component. For example, by tracking the evolution of coherent cyclonic rotating flow regions extracted using this method from atmospheric data on 500-hPa height surfaces, we identify the occurrence of atmospheric blocking phenomena [13]. In oceanography, it is known that the Kuroshio, a flow along the southern coast of Japan, exhibits a meandering phenomenon called the Kuroshio Large Meander (KLM). Extracting the coherent eddy structure due to the meandering from the sea surface height data with TFDA, we have successfully specified the period of KLM, which agrees well with the empirical prediction by the Japan Meteorological Agency. Note that this topological classification theory using COT and COT representations is extended to that for a wide class of vector fields including compressible flows [11], and it is effectively used in the identification of vortex structures for the blood flows in the left ventricle of the heart [10].

In this paper, we extend this topological flow data analysis to Hamiltonian vector fields on  $\mathbb{T}^2$ , so that it is applicable to extracting coherent vortex structures from complex flow patterns in two-dimensional turbulence. Since the flat torus is compact and its topology is different from  $\mathbb{R}^2$ , the original TFDA theory for Hamiltonian flows on  $\mathbb{R}^2$  cannot be applied directly as it is. Since an incompressible vector field on a compact surface can be described locally in terms of differential forms, the particle orbits are affected by the global geometric properties of the surface. As a result, it is impossible to provide a unique Hamiltonian function like  $\mathbb{R}^2$  and to identify its level curves with particle orbits for general curved surfaces. In other words, by using the properties of a manifold, a Hamiltonian function is constructed on a subset of  $\mathbb{R}^2$  as its image for each local coordinate system, and it is impossible to select a single Hamiltonian function. However, in the case of  $\mathbb{T}^2$ , all points can be uniquely represented in a single local coordinate system if we identify this local coordinate system with the  $(x, y)$ -plane and give a Hamiltonian function  $H(x, y)$  defined on it. Hence the particle orbits coincide with the level curves of this Hamiltonian function similar to  $\mathbb{R}^2$ . Another mathematical issue arises when we develop the TFDA theory for the flat torus. In the TFDA theory in  $\mathbb{R}^2$ , the COT is isomorphic to the Reeb graph of the Hamiltonian function. However, the Reeb graph of a function on the torus has one loop, which is not a planar tree. Hence a device is required to convert the topological structures of the Hamiltonian flows on the flat torus into a COT and its associated COT representation.

This paper is structured as follows. Section 2 provides some mathematical preliminaries required to describe our new TFDA theory. In Section 3, we present a topological classification theory for Hamiltonian flows on the flat torus. Based on the classification theory, in Section 3, we describe a conversion algorithm to COTs and COT representations for Hamiltonian flows on the flat torus without physical boundaries, which is essential for practical applications to two-dimensional turbulence. In Section 5, we demonstrate the application of this TFDA method to flow patterns of freely decaying turbulence and enstrophy cascade turbulence. We then show that vortex structures are objectively identified in these flow patterns of turbulence from the viewpoint of topology. Section 6 is a summary. In the Appendix,

we discuss an extension to topological classification theory when the flow domain contains physical boundaries.

## 2. MATHEMATICAL PRELIMINARIES

**2.1. Terms and definitions from the dynamical systems theory.** We consider a two-dimensional compact manifold  $S$  containing physical boundaries. The flow  $v$  on the surface  $S$  is a continuous  $\mathbb{R}$ -action on  $S$ , i.e.,  $v: \mathbb{R} \times S \rightarrow S$ . For the flow  $v$ , we define a mapping  $v_t: S \rightarrow S$  on  $S$  for  $t \in \mathbb{R}$ , where  $v_t(x) := v(t, x)$ . For a point  $x \in S$ ,

$$O(x) = \{v_t(x) \in S \mid t \in \mathbb{R}\}$$

is called an orbit passing through  $x$ . We classify the topological structure of the set of all orbits,  $\{O(x) \mid x \in S\}$ . While the flow  $v$  is an abstract mathematical object, it corresponds to the particle orbits advected by a steady velocity field in analogy with fluid mechanics. Therefore, we will refer to the particle orbits as streamlines unless there is any confusion.

According to the foliation theory [4], it is known that any streamline for a flow  $v$  on a surface  $S$  is classified into either of *proper*, *locally dense*, or *exceptional* in general. In this paper, we assume that streamlines are all proper. This assumption is always satisfied by flow data with finite resolution obtained by numerical simulations or measurements. Hence, it is not a substantial limitation for data analysis. Proper orbits are further classified into three categories: *singular orbits*, *periodic orbits*, and *non-closed orbits*, whose definitions are given as follows.

**Definition 1.** For a proper orbit of the flow,  $v$  on a surface  $S$ , singular orbits, periodic orbits, and non-closed orbits are defined as follows.

- $x \in S$  is a singular orbit if  $x = v_t(x)$  holds for all  $t \in \mathbb{R}$ , namely,  $O(x) = \{x\}$ .
- An orbit  $O(x)$  is periodic if there exists  $T > 0$  such that  $v_T(x) = x$  and  $v_t(x) \neq x$  for  $0 < t < T$ .
- A proper orbit that is neither a singular point nor a periodic orbit is called a non-closed orbit.

The sets of singular points, periodic orbits, and non-closed orbits are denoted by  $\text{Sing}(v)$ ,  $\text{Per}(v)$ , and  $\text{P}(v)$ , respectively.

Let us then recall some mathematical definitions to describe the structures of streamlines of the flow on  $S$ .

**Definition 2.** For a proper orbit through  $x \in S$  of the flow  $v$  on a surface  $S$ , the  $\omega$ -limit set  $\omega(x)$  and the  $\alpha$ -limit set  $\alpha(x)$  are defined as follows.

- $\omega(x) := \bigcap_{n \in \mathbb{R}} \overline{\{v_t(x) \mid t > n\}}$ ; (The set that  $O(x)$  can reach in  $t \rightarrow \infty$ ),
- $\alpha(x) := \bigcap_{n \in \mathbb{R}} \overline{\{v_t(x) \mid t < -n\}}$ ; (The set that  $O(x)$  can reach in  $t \rightarrow -\infty$ ),

where  $\overline{A}$  denotes the closure of the subset  $A \subseteq S$ . Since  $\omega(x)$  and  $\alpha(x)$  are well-defined independently on the choice of a point  $y \in O(x)$ , they are sometimes denoted by  $\omega(O)$  and  $\alpha(O)$ .

A subset of  $S$  is invariant if it is a union of orbits.

## 2.2. Terms and definitions from topology.

**Definition 3.** Let  $I \subset \mathbb{R}$  be an interval.

- (1) A curve on a surface  $S$  is an image of a continuous map  $\gamma: I \rightarrow S$ .

- (2) A curve  $\gamma: [a, b] \rightarrow S$  on a surface  $S$  is said to be simple closed, if  $\gamma(a) = \gamma(b)$  and  $\gamma(s) \neq \gamma(t)$  for every distinct  $s, t \in [a, b]$ .

The particle orbit of the flow  $v$  on  $S$  defines a curve on  $S$ . In particular, a periodic orbit  $O(x)$  with period  $T$  is a simple closed curve  $\gamma: [0, T] \rightarrow S$  owing to  $\gamma(t) = v_t(x)$ .

We now introduce the concepts of *essential* and *inessential* for subsets  $S \subseteq \mathbb{T}^2$  on a torus (or a bounded torus), which plays a vital role in the description of the present theory. Although the two concepts are exclusive, it is easier to understand the definition of inessential subsets first, which paraphrases the equivalent definition in [6, p.348].

**Definition 4.** Let  $S \subseteq \mathbb{T}^2$  be a compact surface. A subset  $E \subseteq S$  is called *inessential* if there exists a pairwise disjoint open covering  $\{D_i\}_{i \in \Lambda}$  of  $E$  (as a set of  $\mathbb{T}^2$ ) such that every  $D_i$  is an open disk. In addition, a subset  $F \subseteq S$  is called *quasi-inessential* if  $\overline{F}$  is inessential.

Then we have the following lemma.

**Lemma 2.1.** For a compact surface  $S \subseteq \mathbb{T}^2$  and a subset  $E \subseteq S$ , the following are equivalent:

- (1) The subset  $E$  is inessential.
- (2) There exists an open neighborhood  $U$  of  $E$  such that every simple closed curve in  $U$  is contractible in  $\mathbb{T}^2$ .
- (3) There exists a disjoint union of open disks in  $\mathbb{T}^2$  which is a neighborhood of  $E$ .

*Proof.* By the uniformization theorem, each connected open surface  $V$  is an open disk if and only if any simple closed curves in  $V$  are contractible. This implies the three assertions are equivalent.  $\square$

An essential set is defined as the negation of an inessential set.

**Definition 5.** Let  $S \subseteq \mathbb{T}^2$  be a compact surface. A subset  $E \subseteq S$  is called *essential* if, for any pairwise disjoint open coverings  $\{D_i\}_{i \in \Lambda}$  of  $E$  (as a set of  $\mathbb{T}^2$ ), there exists  $i_0 \in \Lambda$  such that  $D_{i_0}$  becomes multiply connected. In addition, a subset  $F \subseteq S$  is called *quasi-essential* if  $\overline{F}$  is essential.

By negating each condition in Lemma 2.1, we obtain three equivalent conditions for essential sets. The second condition is easy to understand geometrically.

**Lemma 2.2.** For a compact surface  $S \subseteq \mathbb{T}^2$  and a subset  $E \subseteq S$ , the following are equivalent:

- (1) The subset  $E$  is essential.
- (2) Every open neighborhood  $U$  of  $E$  contains a simple closed curve in  $U$  that is not contractible in  $\mathbb{T}^2$ .
- (3) Every disjoint union of open disks in  $\mathbb{T}^2$  is not a neighborhood of  $E$ .

**Remark 1.** The terms “essential” and “inessential” are well-known in topology. On the other hand, “quasi-essential” and “quasi-inessential” are new technical terms required to describe topological flow properties.

Furthermore, we also introduce a subset of essential sets as follows.

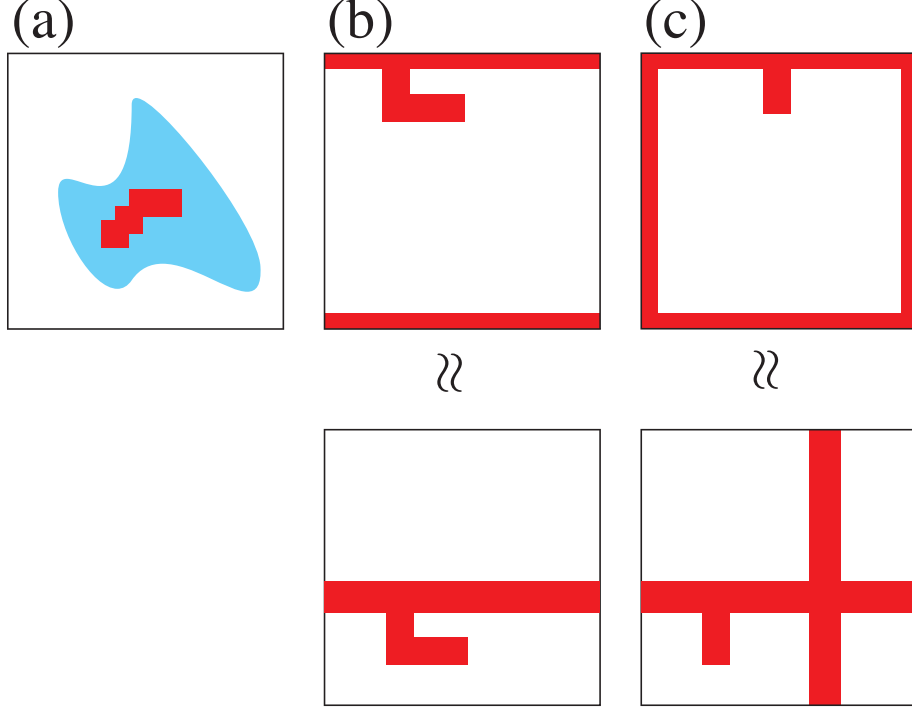


FIGURE 1. The red-filled regions  $U$  are (a) essential, (b) singly essential, and (c) fully essential, respectively. Note that the ones of (b,c) above and below represent the same region under the doubly periodic boundary condition.

**Definition 6.** Let  $S \subseteq \mathbb{T}^2$  be a compact surface. A subset  $E \subseteq S$  is called *fully essential* if its complement  $\mathbb{T}^2 - E$  is inessential.

We can also define sets that are essential but not fully essential.

**Definition 7.** Let  $S \subseteq \mathbb{T}^2$  be a compact surface. When a subset  $E \subseteq S$  is essential but not fully essential, it is called *singly essential*.

**Remark 2.** The term “fully essential” is also well-known in topology. On the other hand, “singly essential” is a new term, since simple closed curves that are “essential” but not “fully essential” appear when we consider sets in a flat torus  $\mathbb{T}^2$ . Hence, we have the following decomposition for a compact surface  $S \subseteq \mathbb{T}^2$ :

$$\begin{aligned} 2^S &= \{\text{inessential subset of } S\} \sqcup \{\text{essential subset of } S\} \\ &= \{\text{inessential subset of } S\} \sqcup \{\text{singly essential subset of } S\} \\ &\quad \sqcup \{\text{fully essential subset of } S\} \end{aligned}$$

Here,  $2^S$  denotes the family of sets consisting of all subsets of  $S$ .

For intuitive understanding, some examples are shown in Figure 1. First, the red-filled region  $U$  in Figure 1(a) is inessential since it is contained in the disk (or its homeomorphic shape). Next, the red subset in Figure 1(b) is singly essential, and

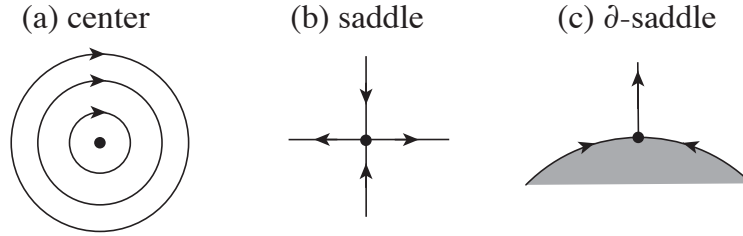


FIGURE 2. Zero-dimensional structures. (a) a center. (b) a saddle. (c) a  $\partial$ -saddle.

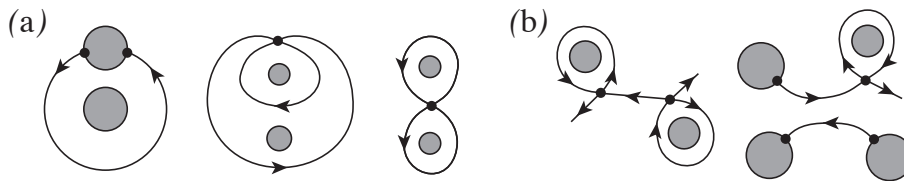


FIGURE 3. Saddle separatrix structures. (a) Self-connected separatrixes. (b) Non-self-connected separatrixes.

its boundary contains an essential simple closed curve. Finally, the fully essential subset in Figure 1(c) crosses both sides of the periodic boundary of the torus. Each component of that boundary is an inessential simple closed curve.

### 3. TOPOLOGICAL CLASSIFICATION OF PARTICLE ORBITS IN HAMILTONIAN FLOWS

**3.1. Local orbit structures.** We introduce local orbit structures in the present topological classification of Hamiltonian flows. We need to consider the topological property of simply closed curves and their flow directions. As explained in the introduction, the Hamiltonian function on a flat torus is represented by a single function,  $H(x, y)$ , where the local coordinate is identified with the  $(x, y)$ -plane. Therefore it is sufficient to consider the local topological structure of particle orbits as level curves of  $H(x, y)$ .

**3.1.1. Zero-dimensional structures.** Figure 2 shows all non-degenerate zero-dimensional singular orbits. A center is a singular orbit with infinitely many periodic orbits around it as shown in Figure 2(a). Figure 2(b) is a saddle associated with two separatrixes. Figure 2(c) is a  $\partial$ -saddle having one separatrix inside the domain and two separatrixes along the boundary.

**3.1.2. One-dimensional structures.** A circuit is an immersion of a set of points or a circle into  $S \subset \mathbb{T}^2$ . The image of a circle under this mapping is either a point or an orbit homeomorphic to the immersed circle. When it is a point, it is called a trivial circuit. It is called a non-trivial circuit when it is an immersed circle. Furthermore, non-trivial circuits are classified into two types. One is a periodic orbit, called a *cycle*, belonging to  $\text{Per}(v)$ . The other is a circuit consisting of saddles in  $\text{Sing}(v)$  and separatrixes in  $\text{P}(v)$ .

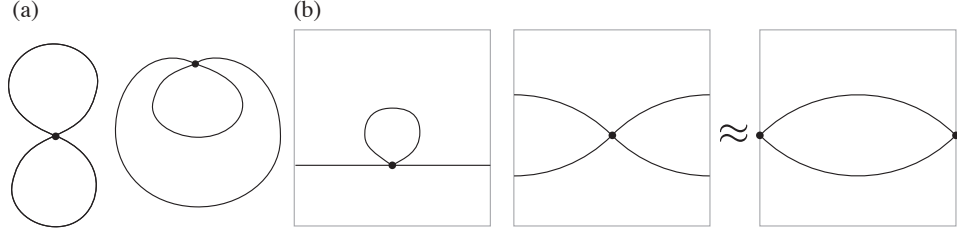


FIGURE 4. One-dimensional structures: saddle connections consist of one saddle and two self-connected saddle separatrices. (a) Inessential saddle connections. (b) Essential saddle connections.

A saddle separatrix is an orbit whose  $\alpha$ -limit set and  $\omega$ -limit set are saddles or  $\partial$ -saddles. Then, the separatrix is said to be connecting and it belongs to  $P(v)$ . When a saddle separatrix connects the same saddle, it is called self-connected. On the other hand, when it connects two different  $\partial$ -saddles on the same boundary, it is called a (self-connected)  $\partial$ -saddle separatrix. Figure 3(a) shows examples of self-connected saddle separatrices. Saddle separatrices connecting different saddles or  $\partial$ -saddles on different boundaries in Figure 3(b) are called non-self-connected saddle separatrices.

A *saddle connection diagram* for a Hamiltonian flow is the set of saddles,  $\partial$ -saddles, and the saddle separatrices connecting them. In particular, a connected component of a saddle connection diagram is called a saddle connection. A saddle connection is said to be self-connected if all saddle separatrices of them are self-connected. The saddle connection diagram is said to be self-connected if it consists of self-connected saddle connections.

Let us consider the simplest non-periodic circuit structures consisting of one saddle and two self-connected saddle separatrices. Figure 4(a) is an inessential saddle connection, and Figure 4(b) shows a singly essential saddle connection. On the other hand, examples of circuits consisting of one boundary, two or more  $\partial$ -saddles, and their self-connected saddle separatrices are a simply essential self-connected saddle connection in Figure 5(a) and a fully essential self-connected saddle connection in Figure 5(b).

**3.1.3. Two-dimensional structure.** An open annulus filled with periodic orbits in  $\text{Per}(v)$  is called a periodic annulus, whose example is shown in Figure 6.

**3.2. Topological structure theorem for the Hamiltonian flows on the flat tours.** A  $C^r$  Hamiltonian vector field  $X$  ( $r \geq 1$ ) on a compact surface is said to be structurally stable if the topological structure of the streamlines does not change when small disturbances are added to the vector field. The exact definition is given as follows.

**Definition 8.** Let  $\mathcal{H}^r(M)$  be the set of  $C^r$ -Hamiltonian vector fields ( $r \geq 1$ ) on a compact surface  $M$ . A  $C^r$ -Hamiltonian vector field  $X$  on  $M$  is said to be structurally stable (in  $\mathcal{H}^r(M)$ ) if any Hamiltonian vector field  $\tilde{X}$  that is  $C^1$ -close to  $X$  is topologically equivalent to  $X$ . That is, there exists a homeomorphism  $h: M \rightarrow M$  such that  $h$  maps the orbits of  $X$  to the orbit of  $\tilde{X}$  without changing the direction of the orbit.



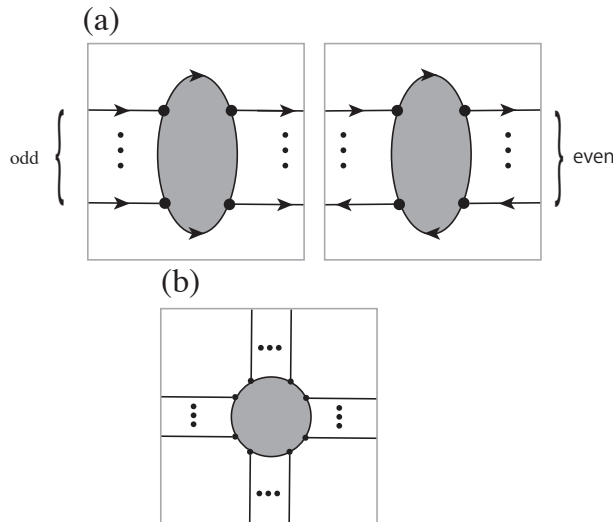


FIGURE 5. One-dimensional structures: Essential saddle connections consisting of one boundary with more than two  $\partial$ -saddles and their self-connected saddle separatrices. (a) Singly essential saddle connections. Note that the orientation of the saddle separatrices varies depending on whether the  $\partial$ -saddle on the boundary is odd or even. (b) Fully essential self-connected saddle connection.

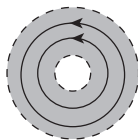


FIGURE 6. Two-dimensional structure: a periodic annulus.

In this paper, a flow generated by a (structurally stable) Hamiltonian vector field is called a (structurally stable) Hamiltonian flow. The following fact about structurally stable Hamiltonian vector fields on compact surfaces is known.

**Theorem 3.1.** [7, Theorem 2.3.8, p. 74] Let  $X$  be a  $C^r$ -Hamiltonian vector field on a compact surface and  $v_X$  the flow generated by  $X$ . Then the following are equivalent:

- (1)  $X$  is structurally stable.
- (2) Any singular orbits of  $v_X$  are non-degenerate and the saddle connection diagram of  $v_X$  is self-connected.

Furthermore, the set of structurally stable  $C^r$ -Hamiltonian vector fields is an open and dense subset of the set of  $C^r$ -Hamiltonian vector fields.

This theorem indicates that the structure of orbits for almost all  $C^r$ -Hamiltonian vector fields is invariant to small perturbations. Furthermore, we state that such a vector field can be decomposed into a finite number of orbit structures in Table 1.

0-dim. structures	saddles, $\partial$ -saddles, centers	Figure 2
1-dim. structures	self-connected saddle separatrices, periodic boundary components	Figure 4
2-dim. structures	open periodic annuli	Figure 6

TABLE 1. Orbit structures appearing in structurally stable Hamiltonian flows.

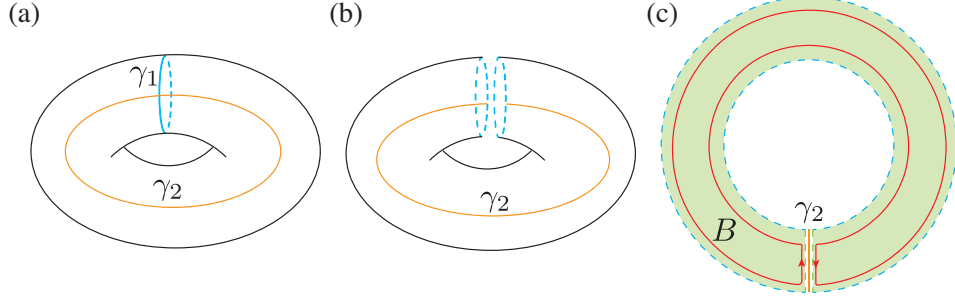


FIGURE 7. (a) A fully essential saddle connection  $C$  on a torus. (b) We remove the essential simple closed curve  $\gamma_1$  from the torus. (c) The open annulus  $A = \mathbb{T}^2 - \gamma_1$  and the open disk  $B = A \setminus C$  are filled with green.

Since the situation is different depending on whether the torus has a boundary or not, we first state the following lemma for a structurally stable Hamiltonian vector field defined on a flat torus  $M$  without physical boundaries.

**Lemma 3.2.** Every saddle connection in a structurally stable Hamiltonian flow on a flat torus without physical boundaries is not fully essential.

*Proof.* Let  $C$  be a saddle connection of the structurally stable Hamiltonian flow on the flat torus  $\mathbb{T}^2$ . Since the flow is structurally stable and the torus contains no physical boundary, the saddle connection  $C$  is self-connected and so it is a union of the saddle and its two connecting separatrices.

We prove it by contradiction. Assume that  $C$  is fully essential as shown in Figure 7(a). Then we choose a saddle separatrix whose closure is an essential simple closed curve  $\gamma_1 \subset C$ . Removing  $\gamma_1$  from the torus, we have an open annulus  $A := \mathbb{T}^2 - \gamma_1$ . Note that the intersection  $A \cap C$  is the other separatrix, say  $\gamma_2$ . See Figure 7(b). Therefore, the set difference  $B := A \setminus C = \mathbb{T}^2 - C$  is an invariant open disk as shown in Figure 7(c). Hence  $C$  is the boundary  $\partial B$  and so is a boundary component of a periodic annulus.

On the other hand, let us consider a periodic orbit near  $\partial B = \gamma_1 \sqcup \gamma_2$ , which appears as a red closed orbit in Figure 7(c). Then, the flow directions of the periodic orbit along both sides of  $\gamma_2$  should be the opposite. However, the flow goes along  $\gamma_2$  in one direction, which is a contradiction.  $\square$

Owing to Lemma 3.2, we determine topologically distinct orbit structures contained in the structurally stable Hamiltonian flows on the torus  $\mathbb{T}^2$  without physical boundaries.

**Proposition 3.3.** The following statements hold for a structurally stable Hamiltonian flow on a flat torus:

- (1) Each self-connected saddle connection is one of the four orbit structures in Figure 4 as an undirected graph up to isotopy on the torus.
- (2) The singular orbits of the Hamiltonian flow are either centers or saddles.

*Proof.* Let  $C$  be a self-connected saddle connection. By Lemma 3.2, the self-connected saddle connection  $C$  is non-fully essential. If  $C$  is inessential, then  $C$  is one of them in Figure 4(a) as an undirected graph up to isotopy on the torus. If  $C$  is singly essential, then  $C$  is one of them in Figure 4(b) as an undirected graph up to isotopy on the torus.  $\square$

On the other hand, if the torus contains physical boundaries, it is possible to have at most one fully essential self-connected saddle connection as shown below.

**Lemma 3.4.** For a structurally stable Hamiltonian flow on the torus with physical boundaries, there exists at most one fully essential saddle connection. Furthermore, if a fully essential saddle connection exists, all other saddle connections are inessential.

*Proof.* As shown in Figure 5(b), a fully essential saddle connection can exist. We will show the uniqueness of a fully essential saddle connection if it exists. Suppose that there exists a fully essential saddle connection  $E$ . By Definition 6, the complement  $\mathbb{T}^2 - E$  is inessential. Any saddle connection except for  $E$  is contained in an invariant open disk  $B \subset \mathbb{T}^2 - E$ . This means that the flow contains no essential saddle connections except the fully essential saddle connection  $E$ .  $\square$

This yields orbit structures of structurally stable Hamiltonian flows on the flat torus with physical boundaries.

**Lemma 3.5.** For a structurally stable Hamiltonian flow on a flat torus with physical boundaries, if the saddle connection diagram contains a singly essential saddle connection, then any other saddle connection is inessential or singly essential.

*Proof.* Let  $C$  be a singly essential saddle connection on a torus. Then,  $\mathbb{T}^2 - C$  consists of an open disk and an essential periodic annulus. Hence, we complete the proof.  $\square$

According to these lemmas, if there exists one singly essential saddle connection then no fully essential saddle connection exists. Conversely, if a fully essential saddle connection exists, then no singly essential saddle connection exists. This is stated in the following dichotomy.

**Corollary 3.6.** One of the following statements holds exclusively for a structurally stable Hamiltonian flow on a flat torus with physical boundaries:

- (1) There exists at most one fully essential saddle connection.
- (2) There exist singly essential saddle connections.

Then the structurally stable Hamiltonian vector field on a flat torus with physical boundaries satisfies the following statement.

**Proposition 3.7.** The following statements hold for a structurally stable Hamiltonian flow on a flat torus with physical boundaries:

- (1) A self-connected saddle connection is either one of the orbit structures in Figure 4, Figure 5, and Figure 17(a) as undirected graph up to isotopy on the surface.
- (2) A fully essential saddle connection contains a physical boundary.
- (3) Any singular orbits of the flow are centers, saddles, or  $\partial$ -saddles.

*Proof.* Let  $v$  be the structurally stable Hamiltonian flow on the flat torus  $S$  with physical boundaries. Then any singular orbit of  $v$  is non-degenerate, i.e., saddles,  $\partial$ -saddles, and centers [2, Theorem 3].

We show a fully essential saddle connection contains a physical boundary by contradiction. Suppose that there exists a fully essential saddle connection and that the orbits near all physical boundaries are periodic orbits. Then by collapsing these physical boundaries into single points, we can make it a structurally stable Hamiltonian flow on a flat torus without physical boundaries. However, Lemma 3.2 implies the non-existence of a fully essential saddle connection, which is a contradiction.

Fix a self-connected saddle connection  $C$ . By Lemma 3.3, if  $C$  contains no  $\partial$ -saddles then  $C$  is one of the four kinds of orbit structures in Figure 4 as undirected graph up to isotopy on the torus. Suppose that  $C$  contains  $\partial$ -saddles. If  $C$  is inessential, then  $C$  is the orbit structure in Figure 17(a). If  $C$  is singly essential, then  $C$  is the orbit structure in Figure 5(a). If  $C$  is fully essential, then  $C$  is the orbit structure in Figure 5(b).  $\square$

#### 4. TREE REPRESENTATION OF TOPOLOGICAL ORBIT STRUCTURES

**4.1. Reeb graph for Hamiltonian flows.** We convert the topological structures of structurally stable Hamiltonian flows on the flat torus into a discrete plane tree, called a partially Cyclically Ordered rooted Tree (COT for short). Let us first introduce the concept of a *finite graph* as follows.

**Definition 9.** A compact Hausdorff space  $G$  is said to be a finite graph if it is a finite one-dimensional cell complex. That is to say, there exists a finite number of points  $v_1, \dots, v_k \in G$  such that  $G - \{v_1, \dots, v_k\}$  is homeomorphic to a finite disjoint union of open intervals.

For a function  $f: X \rightarrow \mathbb{R}$  and  $c \in \mathbb{R}$  on a topological space  $X$ , the inverse image  $f^{-1}(c)$  is called a level set. Furthermore, for a function,  $f: X \rightarrow \mathbb{R}$  on a topological space  $X$ , the space obtained by collapsing the connected components of each level set into a singleton is called the Reeb graph. The space is denoted by  $X/f$ . More precisely, when there exists a connected component  $C$  of  $f^{-1}(c)$  for some  $c \in \mathbb{R}$  such that  $p, q \in C$ , we define the equivalence relation  $p \sim q$ . Then the Reeb graph is represented by  $X/f := X/\sim$ .

**Lemma 4.1.** The Reeb graph of a Hamiltonian function on a compact surface  $S$  with finitely many critical points is a finite graph.

*Proof.* Let  $v$  be a Hamiltonian flow generated by a Hamiltonian function  $H$  on a compact surface. Assume that the Hamiltonian function has only a finite number of critical points. According to [2, Theorem 3], the singular point of  $v$  is either a multi-saddle or a center. Let  $D(v)$  be the saddle connection diagram. The finiteness of  $\text{Sing}(v)$  implies that  $D(v)$  consists of finitely many orbits. Therefore, the complement  $S - (\text{Sing}(v) \cup D(v))$  consists of a finite number of periodic annuli.

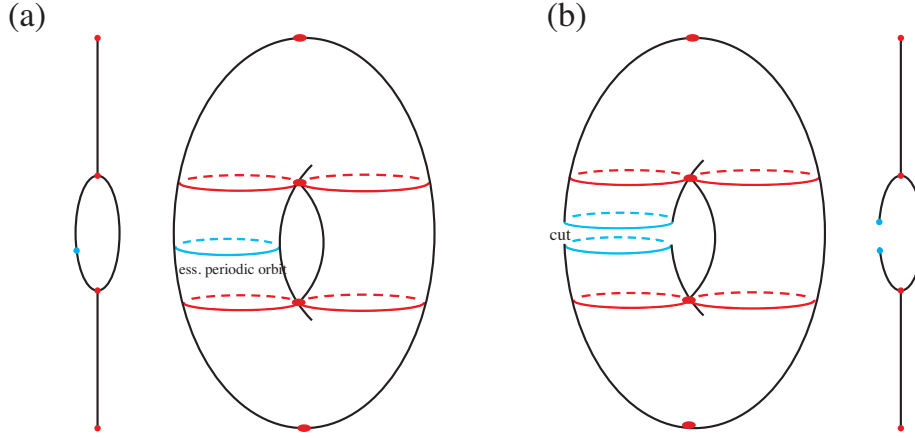


FIGURE 8. (a) Reeb graph for a Hamiltonian function on the torus  $\mathbb{T}^2$ . The Hamiltonian function is split into two at the handle structure of the torus. Then the Reeb graph of the function has a loop structure. (b) When we cut one of the handles along an essential periodic orbit, the Reeb graph of the Hamiltonian function becomes a tree.

As a result, the vertices and edges of the Reeb graph correspond to these singular points and the periodic annuli, respectively.  $\square$

This lemma shows that the Reeb graph of a Hamiltonian function on a compact surface with a finite number of critical points becomes a finite graph.

**4.2. Essential periodic orbit.** The Reeb graph of a continuous function on a torus has a loop structure in general as shown in Figure 8(a) and it is not a tree. To express the topological structure of a given structurally stable Hamiltonian flow on a torus as a tree, we need to introduce *an essential periodic orbit*, which is characterized as follows.

**Lemma 4.2.** For a periodic orbit  $O$  of a Hamiltonian flow on a torus  $\mathbb{T}^2$  without physical boundaries, the following conditions are equivalent:

- (1) The periodic orbit  $O$  is essential.
- (2) The periodic orbit  $O$  does not bound a disk.
- (3) The complement  $\mathbb{T}^2 - O$  is an annulus.

*Proof.* Any sufficiently small  $r$ -neighborhood of  $O$  is homotopic to  $O$ . If  $O$  is essential, then  $\mathbb{T}^2 - O$  is an annulus by definition. If  $\mathbb{T}^2 - O$  is an annulus, then  $O$  does not bound a disk. If  $O$  does not bound a disk, then  $O$  is essential.  $\square$

When the torus contains physical boundaries, we have the following equivalent conditions about an essential periodic orbit:

**Lemma 4.3.** The following conditions are equivalent for a periodic orbit  $O$  of a Hamiltonian flow on a torus  $S$  with physical boundaries:

- (1) The periodic orbit  $O$  is essential.

- (2) The periodic orbit  $O$  does not bound a disk in  $S$ , and it is not parallel to a physical boundary.
- (3) The complement  $S - O$  is an annulus with physical boundaries.

*Proof.* A torus  $S$  with physical boundaries can be considered to be contained in the torus  $\mathbb{T}^2$ . Any sufficiently small  $r$ -neighborhood of  $O$  is homotopic to  $O$ . If  $O$  is essential, then  $S - O$  is an annulus with physical boundaries. If  $S - O$  is an annulus with physical boundaries, then  $O$  does not bound a disk in  $S$  and is not parallel to the boundary. If  $O$  does not bound a disk in  $S$  and is not parallel to the boundary, then  $O$  is essential.  $\square$

These lemmas show that by cutting a torus with an essential periodic orbit as shown in Figure 8(b), we reduce the Hamiltonian flow on a torus with physical boundaries into one on an annulus. Then, for a Hamiltonian function with a finite number of critical points, we can make its Reeb graph into a tree by cutting one edge corresponding to a domain containing an essential simple closed curve from it. Based on this observation, we assume that the Hamiltonian vector field has an essential periodic orbit in what follows. This assumption restricts the class of Hamiltonian vector fields. But, for structurally stable Hamiltonian vector fields on a torus without physical boundary, this condition is always satisfied.

**Lemma 4.4.** Every structurally stable Hamiltonian flow on a torus  $\mathbb{T}^2$  without physical boundaries has essential periodic orbits.

*Proof.* Let  $v$  be a structurally stable Hamiltonian flow on a torus  $\mathbb{T}^2$  and  $H$  be a Hamiltonian function generating  $v$ . By Proposition 3.3, each singular orbit is either a saddle or a center, and each self-connected saddle connection is one of the four orbit structures in Figure 4 as undirected graph up to isotopy on the torus. Therefore, every self-connected saddle connection is inessential or singly essential. From Poincaré–Hopf theorem, since the Euler characteristic of the torus is zero and the index of a saddle (resp. center) is  $-1$  (resp.  $1$ ), the number of saddles equals one of the centers. From Lemma 4.1, the Reeb graph  $G$  of the Hamiltonian  $H$  is a connected finite graph. Moreover, saddles correspond to trivalent vertices and the centers to univalent vertices.

We claim that the Reeb graph  $G$  is not a tree. Indeed, assume that  $G$  is a tree. Since saddles correspond to trivalent (degree-three) vertices and the centers to univalent (degree-one) vertices, by the non-existence of loops in the tree  $G$ , the number of centers is at least two more than the number of saddles, which contradicts the equality of the numbers of centers and saddles.

Since  $G$  is not a tree, the graph  $G$  contains a loop  $K \subset G$ . Then any periodic annuli corresponding to edges in the loop  $K$  are essential. Therefore, so are any periodic orbits contained in the periodic annuli.  $\square$

**Remark 3.** The existence of essential periodic orbits is not necessarily assured when the torus contains physical boundaries. By Corollary 3.6, a structurally stable Hamiltonian flow has either a fully essential saddle connection or a singly essential saddle connection exclusively. For the former case, the Hamiltonian flow has no essential periodic orbit, On the other hand, there exists an essential periodic orbit for the latter case. In this paper, we consider a structurally stable Hamiltonian flow on a torus without physical boundaries. Even if a physical boundary exists, the conversion to COT can be defined similarly as long as an essential periodic orbit

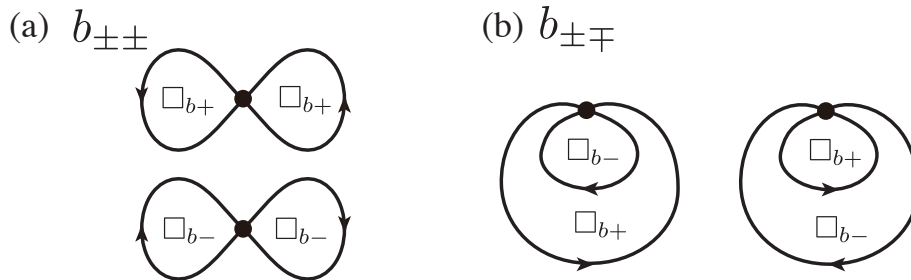


FIGURE 9. One-dimensional orbit structures with a saddle and two quasi-inessential saddle separatrices. (a)  $b_{\pm\pm}$  structures: figure-eight orbit structures. Their COT symbols are given by  $b_{\pm\pm}\{\square_{b_{\pm}}, \square_{b_{\pm}}\}$ . (b)  $b_{\pm\mp}$  structures: orbit structures where one quasi-inessential saddle separatrix encloses another quasi-inessential saddle separatrix. Their COT symbols are given by  $b_{\pm\mp}(\square_{b_{\pm}}, \square_{b_{\mp}})$ .

exists. In the Appendix, we will further discuss the conversion to a COT when the torus contains physical boundaries

**4.3. Root node and current edge.** We can choose any vertex in the graph to be the *root*, but we specify the root in this paper as follows. The Reeb graph  $G$  of the Hamiltonian function becomes a finite graph with exactly one loop as shown in Figure 8(a). Since there exists an essential periodic orbit contained in the structurally stable Hamiltonian flows without physical boundaries, the domain becomes an annulus whose boundary is the essential periodic orbit when we cut the flow domain along the essential periodic orbit. This operation corresponds to cutting one edge of the loop from the Reeb graph  $G$  into disjoint two edges, which yields a tree  $G'$  as shown in Figure 8(b). Then the cut periodic orbit is represented by the two vertices of the graph. We thus choose the root vertex as the lower one, which is a local maximum of the Hamiltonian function in the periodic annulus. Notice that the cutting operation increases by adding one vertex and one edge each. Unless otherwise confused, when the root vertex has degree one, the union of the root and the edges connected to it is also referred to as the *root*.

A *current* is an edge of a rooted tree defined as follows. Let  $G = (V, E)$  be a tree with a root  $v_0 \in V$ . Fix a non-root vertex  $v \in V - \{v_0\}$ . An edge  $e$  of  $G$  is a current of  $v$ , if  $v$  is contained in the boundary of  $e$  and the minimal path from the root to  $v$  contains  $e$ . For the rooted tree  $G'$  of the Reeb graph  $G$  as above, a maximal invariant open periodic annulus that corresponds to the current of a non-root vertex is called a current domain.

**4.4. Local orbit structures and COT symbols.** Based on the topological classification theory in Section 3, we will show that the topological orbit structures for structurally stable Hamiltonian flows with essential periodic orbits can be converted into a COT. Here, with application to two-dimensional turbulent flows in mind, we limit ourselves to Hamiltonian flows on a flat torus without physical boundaries. We then introduce topologically different orbit structures and their corresponding

letters, named COT symbols. See Appendix for additional orbit structures and their COT symbols for Hamiltonian flow on a torus with physical boundaries, to list all possible structures for structurally stable Hamiltonian flows.

**( $\sigma_{\pm}$  structures)** The simplest zero-dimensional local orbit structure is a center shown in Figure 2(a). Since we distinguish flow directions in the topological classification theory, we assign the COT symbol  $\sigma_+$  (resp.  $\sigma_-$ ) for a center having counterclockwise (resp. clockwise) periodic orbits in its neighborhood.

**( $b_{\pm\pm}, b_{\pm\mp}$  structures)** They are one-dimensional orbit structures consisting of a saddle and two quasi-inessential self-connected separatrices as shown in Figure 4(a).

First, for the figure-eight structures in Figure 9(a), we assign the COT symbol  $b_{++}$  (resp.  $b_{--}$ ) when the rotational direction of the two self-connected saddle separatrices is counterclockwise (resp. clockwise). Each saddle separatrix encloses an inner structure symbolized by  $\square_{b_{\pm}}$ , chosen from either of the following statements.

$$(1) \quad \square_{b_+} = \{b_{++}, b_{+-}, \sigma_+\}, \quad \square_{b_-} = \{b_{--}, b_{-+}, \sigma_-\}.$$

Note that the rotational direction of the inner structures is determined by that of the separatrices. In addition, the order of the two inner structures is arbitrary. This situation is expressed as  $b_{++}\{\square_{b_+}, \square_{b_+}\}$  or  $b_{--}\{\square_{b_-}, \square_{b_-}\}$  as the COT symbol.

Next, the COT symbol  $b_{\pm\mp}$  is provided for orbit structures in Figure 9(b), where one quasi-inessential saddle separatrix encloses another quasi-inessential saddle separatrix. When the outer self-connected saddle separatrix is going in the counterclockwise (resp. clockwise) direction, the COT symbol is given by  $b_{+-}$  (resp.  $b_{-+}$ ). Since the rotational direction of the orbit structures inside the separatrices is uniquely determined by definition, its COT symbols are described as  $b_{+-}(\square_{b_+}, \square_{b_-})$  and  $b_{-+}(\square_{b_-}, \square_{b_+})$ , where  $\square_{b_{\pm}}$  denotes the inner structure chosen from (1).

**( $a_{\pm\dot{+}}, a_{\pm\dot{-}}, a_{\dot{+}\dot{-}}, a_{\dot{-}\dot{+}}, \alpha_{\dot{+}\dot{+}}, \alpha_{\dot{-}\dot{-}}, \alpha_{\dot{-}\dot{+}}, \alpha_{\dot{+}\dot{-}}$  structures)** There are one-dimensional structures with one or two quasi-essential saddle separatrices in Figure 4(b), which are characteristic structures of Hamiltonian flows on a torus. The flow domain is divided into three by the saddle separatrices. Hence, ten different COT symbols are assigned depending on the values of the Hamiltonian function in the divided domains as shown in Figure 10.

First, we consider the orbit structure with a quasi-essential saddle separatrix in Figure 4(b). Depending on the flow direction of the quasi-essential saddle separatrix and the current domain, we have six different orbit structures in Figure 10(a)–(f).

- Let us consider the case where the current domain of a saddle connection  $C$  is essential and the intersection of the boundary of the current domain and  $C$  does not contain any inessential simple closed curve. When the Hamiltonian value of the saddle separatrix is higher than that of the current domain as shown in Figure 10(a), we assign the COT symbol  $a_{-\dot{+}}(\square_{b_-}) \cdot \square_{\dot{+}}$  to the orbit structure, in which  $\square_{b_{\pm}}$  denotes inner structures in (1) and  $\square_{\dot{+}}$  is chosen from

$$(2) \quad \square_{\dot{+}} = \{a_{\pm\dot{+}}, \alpha_{+\dot{-}}, \lambda_{\dot{+}}\}.$$

On the other hand, the Hamiltonian value of the saddle separatrices is lower than that of the current domain, we have the orbit structure in Figure 10(b),



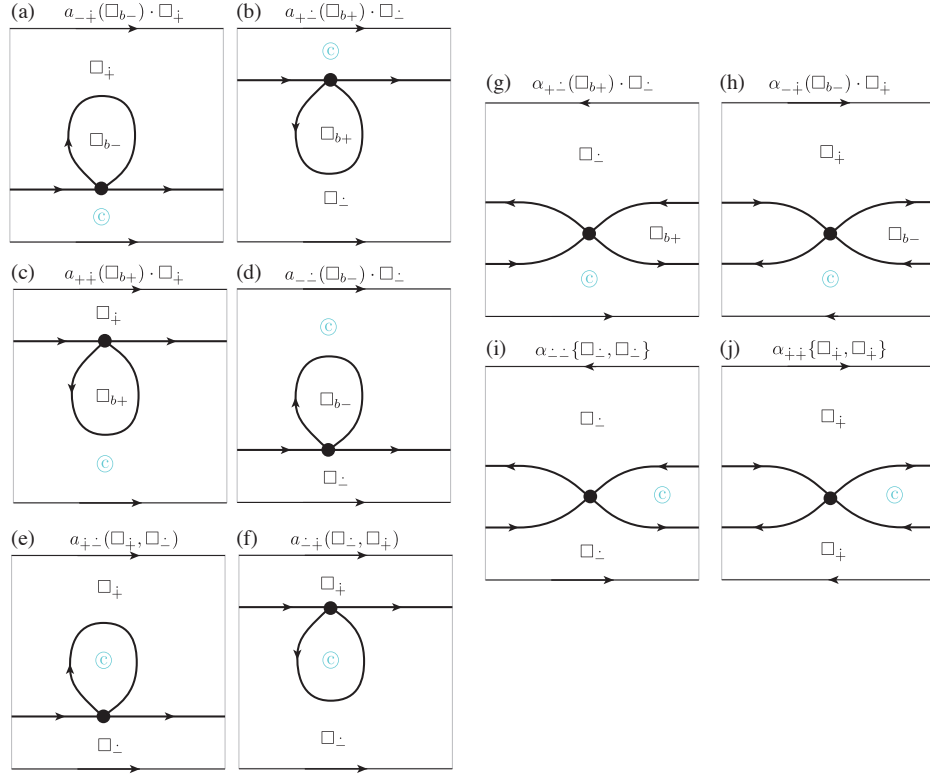


FIGURE 10. One-dimensional orbit structures with quasi-essential saddle separatrices. The symbol  $\odot$  is the location of the current.

whose COT symbol is given by the COT symbol  $a_{+}(\square_{b+}) \cdot \square_{-}$ , in which  $\square_{-}$  is chosen from

$$(3) \quad \square_{-} = \{a_{\pm}, a_{-+}, \lambda_{-}\}.$$

Note that the first and the second components of the subscript of each COT symbol “a” indicate the rotational direction of the inessential simple closed curve and whether the Hamiltonian value of the quasi-essential saddle separatrix is above or below the current domain, respectively.

- Let us consider the case where the current domain of a saddle connection  $C$  is essential and the intersection of the boundary of the current domain and  $C$  contains an inessential simple closed curve. When the Hamiltonian value of the saddle separatrices is higher than that of the current domain, we have the orbit structure in Figure 10(c) and its COT symbol is given by  $a_{++}(\square_{b+}) \cdot \square_{+}$ . On the other hand, when the Hamiltonian value of the saddle separatrices is lower than that of the current domain, the COT symbols of the orbit structure in Figure 10(d) is  $a_{-}(\square_{b-}) \cdot \square_{-}$ .
- Let us consider the case where the boundary of the current domain is inessential. When the Hamiltonian value of the saddle separatrices is higher than that of the current domain, the orbit structure is shown in Figure 10(e) whose COT symbol is given by  $a_{+-}(\square_{+}, \square_{-})$ . When the Hamiltonian value

of the saddle separatrices is lower than that of the current domain as shown in Figure 10(f), the COT symbol  $a_{\cdot\downarrow}(\square_{\cdot}, \square_{\downarrow})$  is assigned to this structure. In these notations, the first and second components of the subscripts of each COT symbol indicate the hierarchical relationship between the area adjacent to the current domain across the one-dimensional inessential simple closed curve, and the hierarchical relationship between the area adjacent to the current at the saddle, respectively.

Next, we consider the orbit structure with two quasi-essential saddle separatrices on the right of Figure 4(b). Then, depending on the current domain and the hierarchical structure of the Hamiltonian values, we have the following four different orbit structures in Figure 10(g)–(j).

- Suppose that the current domain of a saddle connection  $C$  is essential. When the Hamiltonian values of the current domain are lower than that of the saddle connection  $C$ , we have the orbit structure of Figure 10(g) whose COT symbol is given by  $\alpha_{+\cdot}(\square_{b+}) \cdot \square_{\cdot}$ . On the other hand, the Hamiltonian values of the current domain are higher than that of the saddle connection  $C$ , so we have the orbit structure of Figure 10(h) and its COT symbol is given by  $\alpha_{-\downarrow}(\square_{b-}) \cdot \square_{\downarrow}$ .
- Suppose that the current domain of a saddle connection  $C$  is inessential. When the Hamiltonian values of the current domain are higher than that of the saddle connection  $C$ , we have the orbit structure of Figure 10(i) whose COT symbol is given by  $\alpha_{\cdot\cdot}(\square_{\cdot}, \square_{\cdot})$ . On the other hand, when the Hamiltonian values of the current domain are lower than that of the saddle connection  $C$ , we have the orbit structure of Figure 10(j) and its COT symbol is given by  $\alpha_{\downarrow\downarrow}(\square_{\downarrow}, \square_{\downarrow})$ .

**( $\beta_{\pm}$  structures)** This one-dimensional orbit structure corresponds to a boundary component of the annular region. When the torus is cut by the essential periodic orbit and divided into an annular region, we assign the COT symbol  $\beta_{\downarrow}$  (resp.  $\beta_{\cdot}$ ) to the boundary components of the region with lower (resp. higher) Hamiltonian values as viewed from the essential periodic orbit. By construction, the COT for any Hamiltonian flow on a torus has a pair of  $\beta_{\downarrow}$  and  $\beta_{\cdot}$ . Furthermore, by identifying the essential periodic orbits  $\beta_{\downarrow}$  and  $\beta_{\cdot}$ , the Reeb graph of the Hamiltonian flow on the torus with one cycle is recovered.

**4.5. Conversion to COT.** Recall that we assume the existence of an essential periodic orbit in a structurally stable Hamiltonian flow on a torus. If we cut the torus along the periodic orbit, then the Hamiltonian flow on the torus is transformed into a Hamiltonian flow on a closed annulus. For Hamiltonian flows on the annulus, it is possible to use the existing conversion algorithm to COT developed in [14]. Hence, we have only to specify how to extract an essential periodic orbit. Here, we employ a method to extract a periodic orbit closest to the minimum point of the Hamiltonian function by considering the direction of the first homology class, which is explained below.

Let  $\widehat{H}: \mathbb{R}^2 \rightarrow \mathbb{R}$  be a  $C^1$  function on  $\mathbb{R}^2$  which is doubly periodic. That is to say, for any  $x, y \in \mathbb{R}^2$  and  $m, n \in \mathbb{Z}$ ,  $\widehat{H}(x + m, y + n) = \widehat{H}(x, y)$  holds. Then, a Hamiltonian function  $H: \mathbb{T}^2 \rightarrow \mathbb{R}$  on the torus  $\mathbb{T}^2 := \mathbb{R}^2/\mathbb{Z}^2$  is induced. We then investigate the topological orbit structure of the Hamiltonian vector field  $X_H$  on  $\mathbb{T}^2$ . Suppose local coordinates are induced from  $\mathbb{R}^2$  before taking the quotient set.

Note that this assumption corresponds to how we determine the origin of a torus for a given data set in the context of data analysis. We set the origin at the bottom left point of the coordinate system, and we define the  $x$ -axis as the horizontal direction and the  $y$ -axis as the vertical direction.

4.5.1. *Conversion algorithm to COT.* Suppose that we choose the root as an essential periodic orbit on the boundary as in Section 4.3. The procedure assigning a COT and a COT representation for a given Hamiltonian function generating a structurally stable Hamiltonian flow on a torus is described as follows.

- : **(Step 1)** We consider all sublevel sets that contain the local minimums of the Hamiltonian function. We then find the boundaries of the sublevel sets containing an essential simple closed curve which has a minimal Hamiltonian value among such essential simple closed curves.
- : **(Step 2)** Since there exist essential periodic orbits near the essential simple closed curve chosen by (Step 1) on both sides of the level set, we uniquely choose an essential periodic orbit according to procedure (P) described in Section 4.5.2.
- : **(Step 3)** Cut the torus along this essential periodic orbit  $O$  and transform it into an annular region.
- : **(Step 4)** We set the initial current domain as the domain one whose boundary component is  $O$  and where the value of the Hamiltonian function is smaller than that of the essential periodic orbit  $O$ . Starting from the current domain, we construct a COT according to the existing conversion algorithm for Hamiltonian flows on the annulus [14]. Then we assign the COT symbol  $\beta_{\dagger}$  for the vertex corresponding to the boundary essential periodic orbit.
- : **(Step 5)** Starting from the root vertex  $\beta_{\dagger}$ , we derive the COT representation for the COT.

We note that the essential simple closed curve chosen by this algorithm is always contained in the local orbit structure of  $\alpha_{-\dagger}$  in Figure 10(h) as shown in the following lemma.

**Lemma 4.5.** Every essential simple closed curve chosen by the algorithm contains a quasi-essential saddle separatrix whose corresponding COT symbol is  $\alpha_{-\dagger}$ .

*Proof.* Let  $H$  be a Hamiltonian function generating a structurally stable Hamiltonian flow on a torus without physical boundaries. In Step 1, the algorithm chooses a closed sublevel set  $\Gamma$  that contains the local minimums of the Hamiltonian function and saddles not in its interior but on the boundary. Then the boundary component  $\gamma$  in  $\Gamma$  is the local minimum in essential connected components of levelsets near  $\gamma$ . By construction of  $\Gamma$ , the sublevel set  $\Gamma$  contains a local minimum but no local maximum. This implies that the quasi-essential separatrix  $\mu$  in  $\gamma$  appears in Figure 10(a,d,e,h,j).

Assume the quasi-essential separatrix  $\mu$  in  $\gamma$  appears as in Figure 10(a,d,e). We then consider the subdomain consisting of essential level sets there. The values of the Hamiltonian function are monotonically decreasing in the subdomain from top to bottom. Hence, any values of the Hamiltonian function in the subdomain are not minimal. This implies that the quasi-essential saddle separatrix  $\mu$  is not minimal in the subdomain, which contradicts the local minimality of  $\gamma$  containing the quasi-essential saddle separatrix  $\mu$ . Thus the quasi-essential separatrix  $\mu$  is contained as in Figure 10(h,j).

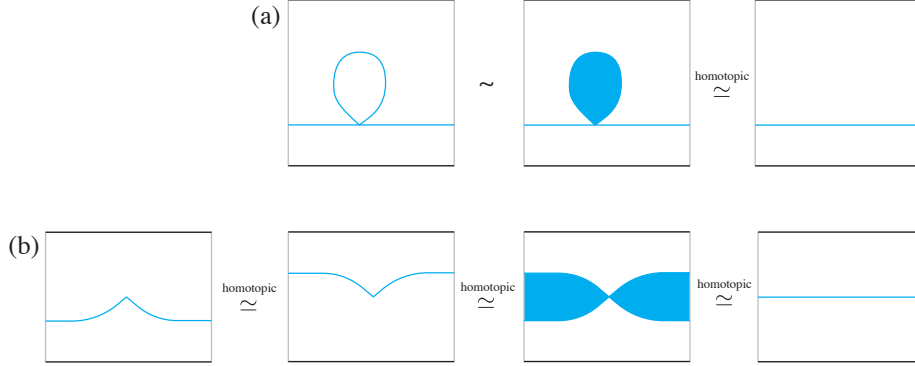


FIGURE 11. First homology class of saddle connections for the local orbit structures (a)  $a_{-\pm}$  and (b)  $\alpha_{+\pm}$ . The symbol  $\sim$  means that the subgroups in  $H_1(\mathbb{T}^2)$  induced by the inclusions coincide with each other and are generated by one generator.

Finally, in Figure 10(h,j), since  $\gamma$  is the local minimum, Step 3 makes a current domain essential in the original surface  $S$ . Therefore, the one-dimensional structure  $\alpha_{-\pm}$  of Figure 10(h) only satisfies the locally minimal condition of  $H$  and the position of the current simultaneously.  $\square$

4.5.2. *Procedure (P) determining a unique essential periodic orbit.* We explain the procedure of choosing an essential periodic orbit uniquely for the local orbit structure having two quasi-essential saddle separatrices of  $\alpha_{-\pm}$ . Let us recall some mathematical terms and known facts before providing the procedure.

Consider the local orbit structure of  $a_{-\pm}$  in the top left of Figure 11(a). When we fill the disk bounded by the inessential saddle connection  $C$ , the saddle connection  $C$  and its filling  $F_C$  are homologous and belong to the same homology class. More precisely, the first homologies induced by inclusions  $C \rightarrow S$  and  $F_C \rightarrow S$  are isomorphic and are generated by one element respectively. Furthermore, the generators are the same homology class except for the sign as one essential simple closed curve on the right panel of Figure 11(a). Similarly, as shown in Figure 11(b), the two essential simple closed curves in the local orbit structure of  $\alpha_{-\pm}$  are homologous to the one obtained by filling a contractible disk region between saddle connections. Hence, they all belong to the same homology class as the essential simple closed curve in the rightmost ones of Figure 11(a,b). On the other hand, every simple closed curve  $\gamma$  in the torus  $\mathbb{T}^2 := \mathbb{R}^2/\mathbb{Z}^2$  is generally winding  $k$  times horizontally and  $l$  times vertically as an undirected circuit. More precisely, a simple closed curve  $\gamma$  defines the projection class  $[(k, l)] \in (\{0\} \times \mathbb{Z}_{>0}) \sqcup (\mathbb{Z}_{>0} \times \mathbb{Z}) \cong (\mathbb{Z}^2 - \{0\})/\pm \cong (H_1(\mathbb{T}^2; \mathbb{Z}) - \{0\})/\pm$  of the first homology class. In particular,  $a_{-\pm}$  and  $\alpha_{-\pm}$  in Figure 11(a,b) define the first homology class corresponding to  $[(1, 0)]$ .

By using these terms, the procedure (P) for defining an essential periodic orbit is now precisely described as follows: The projection class of the first homology class for the essential simple closed curve  $\gamma$  in the saddle connection of  $\alpha_{-\pm}$  pattern in Figure 12 is  $[(k, l)] = [(1, 0)]$ . Therefore, the essential periodic orbit is chosen by translating in a direction perpendicular to the  $[(k, l)]$  direction within the level set

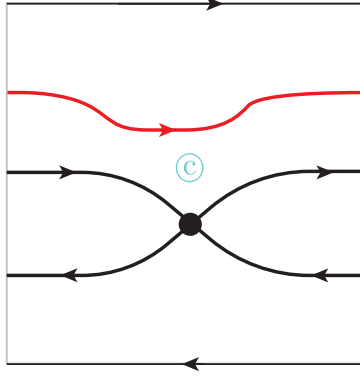


FIGURE 12. An essential periodic orbit (a level curve of the Hamiltonian function) near the saddle connection of the local orbit structure  $\alpha_{-+}$ .

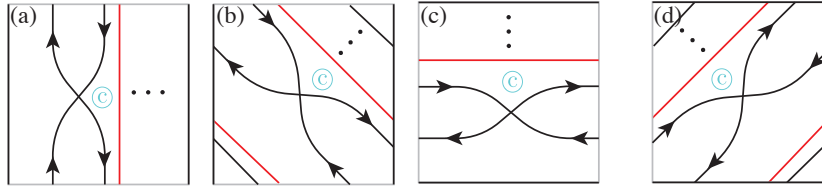


FIGURE 13. First homology class of saddle connection

near  $\gamma$  shown as the red orbit in Figure 12. Here we note that there are two choices of essential simple closed curves as shown in the two left panels of Figure 11. On the other hand, regardless of which of these two is chosen, the same projection class of the first homology class is determined. Hence, for the saddle connection  $\gamma$  with  $[(k, l)] \in (\{0\} \times \mathbb{Z}_{>0}) \sqcup (\mathbb{Z}_{>0} \times \mathbb{Z})$ , we define an essential periodic orbit as follows.

- (1) For  $k = 0$ , since the essential simple closed curve doesn't wind horizontally, and the simple closed curve  $\gamma$  has no self-intersection, we have  $[(k, l)] = [(0, 1)]$  as shown in Figure 13(a). Then, we choose a level set near  $\gamma$  shifted along the  $x$ -axis as an essential periodic orbit.
- (2) For  $k > 0$ , as shown in Figure 13(b,c,d), we choose a level set near  $\gamma$  shifted along the  $y$ -axis as essential periodic orbit.

**Remark 4.** Note that the essential periodic orbit extracted by this procedure is not continuous for the choice of projection class for the first homology class.

4.5.3. *Existence of the conversion algorithm.* We now obtain the following theorem.

**Theorem 4.6.** There is an algorithm for converting any structurally stable Hamiltonian flow in the flat torus with a boundary and an essential periodic orbit into a COT representation.

*Proof.* Fix any structurally stable Hamiltonian flow  $v$  in the flat torus with a boundary and an essential periodic orbit. Since the flow  $v$  contains an essential periodic orbit, we can choose an essential periodic orbit owing to the procedure (P). By

cutting the torus along the chosen essential periodic orbit, the resulting flow is a structurally Hamiltonian flow on a punctured closed annulus. In addition, we have established the algorithm for converting the topological structures of particle orbits for structurally stable Hamiltonian flows in punctured closed annuli into a COT and a COT representation [15, 16]. Hence, the conversion algorithm is well-defined.  $\square$

**Remark 5.** The algorithm gives a COT that depends on the choice of the essential periodic orbit. The COT is independent of how we choose the essential periodic orbit in the same periodic annulus. On the other hand, as discussed in procedure (P), we have two different periodic annuli where essential periodic orbits are contained. Hence, we have a different COT when we choose the different annular regions. However, since the Reeb graph of the Hamiltonian function with a loop before cutting is the same, we could convert between these COTs.

### 5. TOPOLOGICAL VORTEX STRUCTURES IN TURBULENT FLOWS

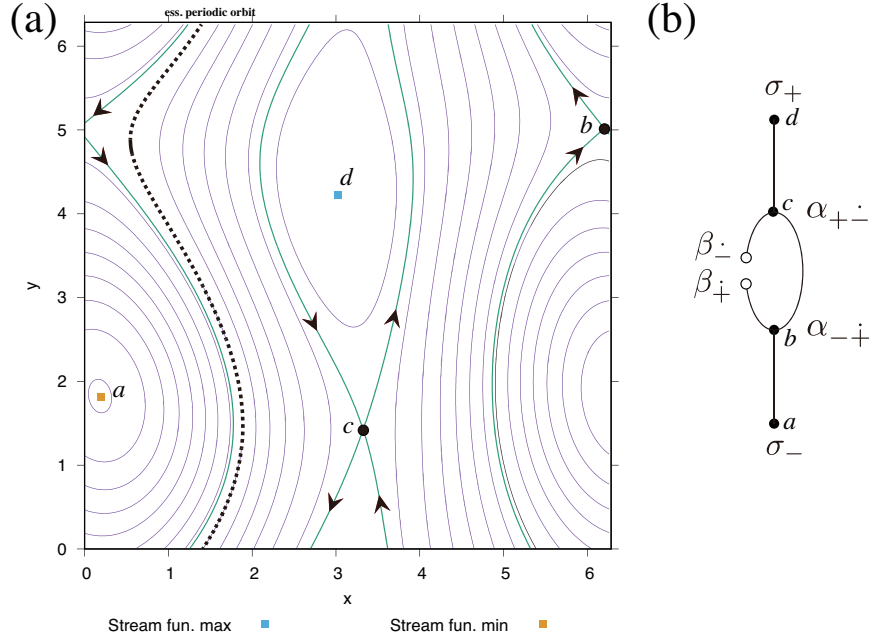


FIGURE 14. (a) A snapshot of level curves of the stream function of two-dimensional free decaying turbulence in a doubly periodic domain. The dashed level curve is the essential periodic orbit extracted by the procedure (P). (b) The COT for the Hamiltonian flow with the stream function being its Hamiltonian function. Its COT representation is (4).

**5.1. Application of TFDA to 2-D turbulent flows.** We consider some applications of the present conversion algorithm to two-dimensional free decaying turbulence and enstrophy cascade turbulence in a doubly periodic domain. The stream function is the Hamiltonian function for the flows.

Figure 14(a) shows a snapshot of level curves of the stream function of freely decaying turbulence. Let us obtain the unique COT and the COT representation for this flow according to the algorithm. Since the concept of left and right cannot be determined for the flow inside a torus, we define up, down, left, and right as shown in this figure for the sake of description. First, to determine the essential periodic orbit, we find the point where the Hamiltonian function becomes the minimum, which is the center  $a$  shown as the yellow box in the figure. We then set the current domain in the sublevel set that contains the minimum point between the two quasi-essential saddle separatrices of the saddle  $b$ . Since the boundary of this sublevel set is the two saddle separatrices with the saddle  $b$ , we choose an essential periodic orbit from the right to the right of  $b$ , along which we cut the torus. Since the value of the Hamiltonian function in the region to the left of this periodic orbit is lower, we provide the COT symbol  $\beta_{\dot{+}}$  to the boundary periodic orbit and set the initial current to this region. Starting with this current, we construct the COT, i.e., the Reeb graph of the Hamiltonian flows as follows.

First, it follows from the current domain and the directions of the saddle separatrices of the saddle  $b$  that the topological structure that appears is the one shown in Figure 10(h). Hence, we assign the COT symbol  $\alpha_{-\dot{+}}(\square_{b-}^1) \cdot \square_{\dot{+}s}^1$  to this structure. The inner structure of  $\alpha_{-\dot{+}}$  is the elliptic center  $a$ , and it is represented by  $\square_{b-}^1 = \sigma_-$ . Next, we move the current to the domain corresponding to the structure of  $\square_{\dot{+}s}^1$ . For this current, the next topological structure is the saddle  $c$  with two quasi-essential saddle separatrices. From the configuration of the current domain and the direction of the saddle separatrices of  $c$ , the local orbit structure is equivalent to the one in Figure 10(g). Hence, we have  $\square_{\dot{+}s}^1 = \alpha_{+\dot{-}}(\square_{b+}^2) \cdot \square_{\dot{-}s}^2$  in which the inner structure is the elliptic center  $d$  with  $\square_{b+}^2 = \sigma_+$ . Finally, the region to the left of the saddle  $c$  has the boundary essential periodic orbit, which is the end of the structure. Consequently, we assign  $\square_{\dot{-}s}^2 = \beta_{\dot{-}}$  to the essential boundary periodic orbit. The COT (Reeb graph) is shown in Figure 14(b) whose COT representation is given by

$$(4) \quad \beta_{\dot{+}} \cdot \alpha_{-\dot{+}}(\sigma_-) \cdot \alpha_{+\dot{-}}(\sigma_+) \cdot \beta_{\dot{-}}.$$

The next application is the level curves of the stream function for an enstrophy cascade turbulence as shown in Figure 15. The yellow box (resp. the orange box) on the left of the figure represents the minimum point (resp. the maximum point) of the stream function. This flow has three saddles (①–③) with quasi-essential saddle separatrices and seven saddles ( $a$ – $g$ ) with quasi-inessential self-connected saddle separatrices only. Since the saddle separatrices are densely located in a very narrow region, we extract the saddle connection diagram schematically in Figure 16(a) to make it easy to apply the conversion algorithm. Using this schematic figure, we construct the COT as follows.

First, since the flow around the yellow point where the minimum value is located is clockwise, its COT symbol is  $\sigma_-$ . From there, searching sublevel sets containing the minimum point toward higher values of the Hamiltonian function, we find the saddle ② with quasi-essential saddle separatrices. Following procedure (P), we choose an essential periodic orbit in the upper region, which is drawn as a dashed curve, and cut the region along the orbit. We assign the COT symbol  $\beta_{\dot{+}}$  to the essential periodic orbit that is the boundary of the region with lower values of the Hamiltonian function, and set the initial current to the region. The next

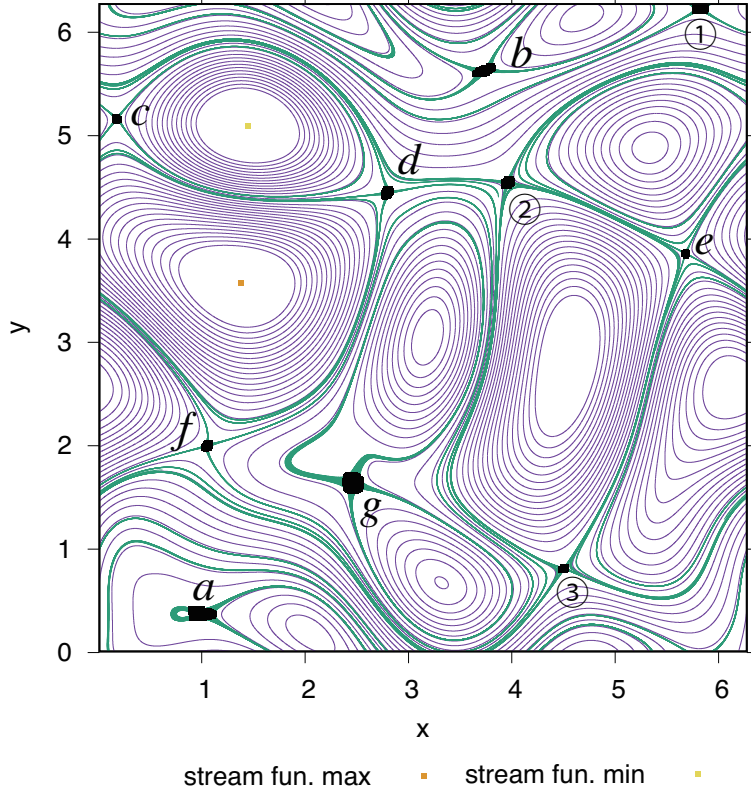


FIGURE 15. A snapshot of the level curves of the stream function of two-dimensional enstrophy cascade turbulence.

topological orbital structure we find for this current domain is the saddle ② with two quasi-essential saddle separatrices whose configuration is equivalent to Figure 10(h). Hence, the COT symbol for this structure is given by  $\alpha_{-+}(\square_{b-}^1 \cdot \square_{b+}^1)$ . The inner structure  $\square_{b-}^1$  of  $\alpha_{-+}$  is the saddle  $e$  having the COT symbol  $b_{-+}(\square_{b-}^2, \square_{b+}^2)$ . Since the inner structure for  $\square_{b+}^2$  is the elliptic center having the maximum Hamiltonian value, we have  $\square_{b+}^2 = \sigma_+$ . For the inner structure  $\square_{b-}^2$ , we find the saddle  $d$  with the COT symbol  $b_{--}\{\square_{b-}^3, \square_{b-}^4\}$ . In a similar manner, checking the inner structure  $\square_{b-}^3$ , we find a nested structure of the saddle  $f$  and  $g$  with the COT symbol  $b_{--}$ . On the other hand, for the inner structure for  $\square_{b-}^4$ , we have one saddle  $c$  with the COT symbol  $b_{--}$ .

Now that we have extracted all of the structure for  $\square_{b-}^1$ , we move the current to the region of  $\square_{b+}^1$  below the saddle ②. Then we search the topological structures toward higher values of the Hamiltonian function and find the saddle ③ having one quasi-essential saddle separatrix and one counterclockwise quasi-essential saddle separatrix whose configuration corresponds to Figure 10(c). The COT symbol for this topological orbit structure of the saddle ③ is given by  $a_{++}(\square_{b+}^5 \cdot \square_{+s}^5)$ . Since  $\square_{b+}^5$  corresponds to the region containing an elliptic center  $\sigma_+$ , the search terminates and  $\square_{b+}^5 = \sigma_+$ . We move the current to the other region of  $\square_{+s}^5$  and search the



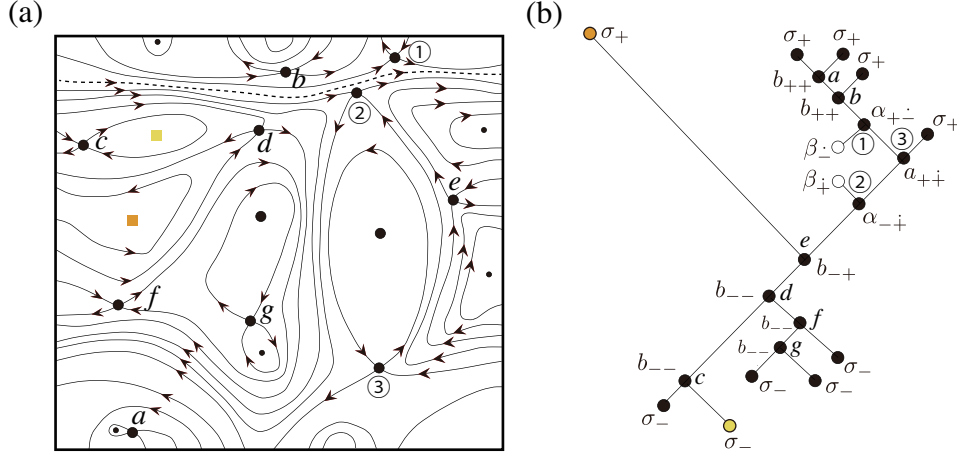


FIGURE 16. (a) The saddle connection diagram extracted schematically from the level curves of the stream function in Figure 15. (b) The COT for the saddle connection diagram. Its COT representation is given by (5).

topological orbit structures toward higher values of the Hamiltonian function. We find the saddle ① with quasi-essential saddle separatrices whose configuration is equivalent to Figure 10(g) associated with the COT symbol  $\alpha_{+\pm}(\square_{b_+}^6) \cdot \square_{-s}^6$ . For the structure  $\square_{-s}^6$ , we find the essential periodic orbit  $\square_{b_-}^6 = \beta_-$  and the search in this direction ends. Finally, searching the topological orbit structure toward higher values of the Hamiltonian function for  $\square_{b_+}^6$ , we have a nested structure of the saddles  $a$  and  $b$  with the COT symbol  $b_{++}$ . Since all topological orbit structures are detected, we have the COT for the Hamiltonian flows as in Figure 16(b). Its COT representation is finally described by

$$(5) \quad \beta_{+\pm} \cdot \alpha_{-\pm}(b_{-+}(b_{--}\{b_{--}\{\sigma_-, \sigma_-\}, b_{--}\{b_{--}\{\sigma_-, \sigma_-\}, \sigma_-\}\}, \sigma_+)) \\ \cdot a_{+\pm}(\sigma_+) \cdot \alpha_{+\pm}(b_{++}\{b_{++}\{\sigma_+, \sigma_+\}, \sigma_+\}) \cdot \beta_{-\pm}.$$

**5.2. Detection of topological vortex structures via TFDA.** Based on the COTs and COT representations of streamline patterns, we here propose a method for extracting coherent swirling flow regions in 2d turbulence as topological vortex structures.

Let us first consider the local orbit structures represented by the COT symbols,  $b_{\pm\pm}$ ,  $b_{\pm\mp}$  in Figure 9, and  $a_{\pm\pm}$ ,  $a_{\pm\mp}$  in Figure 10(a)–(f). The region enclosed by the quasi-inessential saddle separatrix in these structures represents the swirling flow region, which we define as a *topological vortex structure*. Note that this structure does not always coincide with the high vorticity region. Next, the local orbit structures with the COT symbols  $\alpha_{\pm\mp}$  and  $\alpha_{\pm\pm}$  in Figure 10(g)–(j) have two quasi-essential saddle separatrices, enclosing an inessential swirling flow region with large scales of the doubly periodic flow domain. Since such a region is an artificial structure originating from doubly periodic boundary conditions, it is not regarded as a topological vortex structure.

On the other hand, the two quasi-essential saddle separatrices of the local orbit structures  $\alpha_{\pm\mp}$  and  $\alpha_{\pm\pm}$  divide the whole flow domain into two subdomains: an inessential rotational flow domain and an essential uniform flow domain. Thus we call it a *topological partitioning structure*. The essential rotating flow domain obtained by this partition can contain topological vortex structures associated with the local orbit structures  $b_{\pm\pm}$  and  $b_{\pm\mp}$ . On the other hand, the essential uniform flow region could contain topological vortex structures enclosed by a quasi-essential saddle separatrix of the local orbit structures  $a_{\pm\pm}$  and  $a_{\pm\mp}$ . From this point of view, the former topological vortex structures are called *entrapped* and the latter be *translating*.

We use these concepts to identify topological vortex structures from the two streamline patterns of 2d turbulence considered in §5.1. First, the COT representation (4) of the flow pattern of free decaying turbulence in Figure 14 indicates that there are two topological partitioning structures represented by  $\alpha_{-\dot{+}}$  and  $\alpha_{+\dot{-}}$ , but no topological vortex structures exist here. According to the COT for the flow pattern of enstrophy cascade turbulence in Figure 16(b) and the COT representation (5), the essential domain defined by the topological partitioning structure of  $\alpha_{-\dot{+}}$  corresponding to the saddle ② includes entrapped topological vortex structures associated with the saddles  $c, d, e, f$  and  $g$ . In particular, the regions corresponding to the leaves of the COT connected to nodes  $c, f, e$ , and  $g$  represent coherent topological vortex structures. On the other hand, the  $\alpha_{+\dot{-}}$  structure corresponding to the saddle ③ has a large translating counter-clockwise topological vortex structure. In addition, the region partitioned by the topological partitioning structure  $\alpha_{+\dot{-}}$  of the saddle ① contains three coherent topological structures corresponding to the saddles  $a$  and  $b$ . In this way, the COTs and the COT representation obtained by TFDA enable us to objectively extract the vortex structures in two-dimensional turbulence from the viewpoint of topology.

## 6. SUMMARY

We have developed a topological classification theory for the orbit structures of structurally stable Hamiltonian flows on a flat torus. Structurally stable Hamiltonian flows can have quasi-essential saddle separatrices such as Figure 4(b), which differs from structurally stable Hamiltonian flows in the plane. In particular, a fully essential saddle connection with multiple  $\partial$ -saddles in a physical boundary can exist. This is a topologically characteristic feature of flows on the torus when it contains physical boundaries.

Based on this classification theory, we show that the topological streamline structure of structurally stable Hamiltonian flows is converted into a partially cyclically ordered rooted tree (COT) when a torus has no physical boundaries. The conversion algorithm is described as follows. First, we reduce the Hamiltonian flow on the torus to a Hamiltonian flow on an annulus by cutting a handle of the torus along an essential periodic orbit. We then apply the conversion algorithm for structurally stable Hamiltonian flows on the annulus developed in [14]. The COT depends on this cut periodic orbit in general. We note that we remove the loop from the Reeb graph of the Hamiltonian function by cutting the torus, but two new nodes representing this periodic orbit are added to the COT. On the other hand, the Reeb graph can be reproduced by identifying two nodes of the COT.

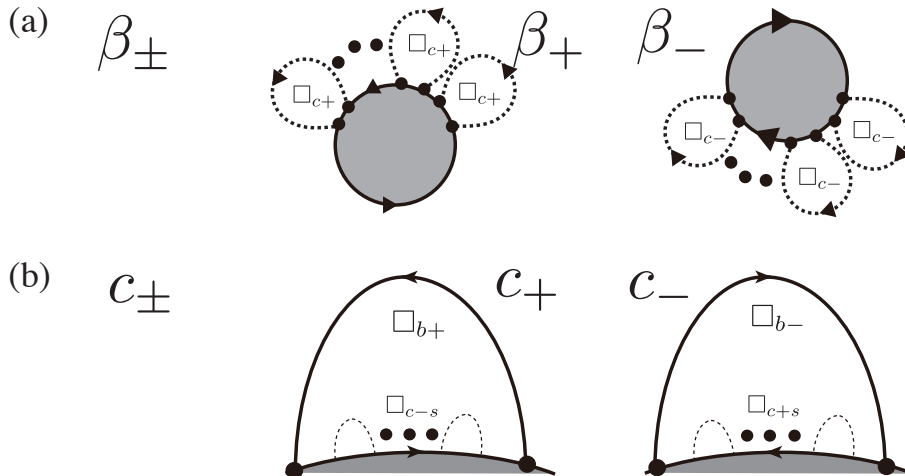


FIGURE 17. One-dimensional structures with inessential self-connected boundary saddle separatrices. (a)  $\beta_{\pm}$  structure: A physical boundary with any number of inessential  $\partial$ -saddle separatrices. When the flow direction along the boundary is counter-clockwise (resp. clockwise), its COT representation is  $\beta_{+}\{\square_{c+s}\}$  ( $\beta_{-}\{\square_{c-s}\}$ ). (b)  $c_{\pm}$  structures: A one-dimensional structure with any number of  $\partial$ -saddle separatrices filled with periodic orbits inside. The COT symbol is given by  $c_{\pm}(\square_{b_{\pm}}, \square_{c_{\mp s}})$ .

Finally, we apply the conversion algorithm to snapshots of freely decaying turbulence and enstrophy cascade turbulence over a planar domain with a doubly periodic boundary condition. Owing to this COT representation of the flows, coherent topological vortex structures are extracted as regions bounded by self-connected saddle separatrices. We examine the statistics of such coherent vortex structures and their mutual interactions to characterize two-dimensional turbulence from the viewpoint of topology. This investigation will be reported shortly.

#### APPENDIX A. LOCAL ORBIT STRUCTURES OF HAMILTONIAN FLOWS ON A FLAT TORUS WITH PHYSICAL BOUNDARIES AND THEIR COT SYMBOLS

In this paper, aiming at the applications to two-dimensional fluid turbulence in a doubly periodic domain, we have developed the conversion algorithm for Hamiltonian flows on the torus without physical boundaries. However, this is not an essential restriction. We can obtain a similar conversion algorithm to COT and COT representations even if the flow domain contains physical boundaries. In the Appendix, we provide the topological classification of local orbit structures in Hamiltonian flows on a torus with physical boundaries and their COT symbols for reference although we won't give the conversion algorithm.

**A.1. Local orbit structures with only inessential saddle connections. ( $\beta_{\pm}$  structures)** This one-dimensional structure corresponds to a physical boundary with an arbitrary number of  $\partial$ -saddle separatrices as shown in Figure 17(a). When there exist  $\partial$ -saddle separatrices on the boundary and the flow direction along

the boundary is counter-clockwise (resp. clockwise), the COT symbol is given as  $\beta_+\{\square_{c+s}\}$  (resp.  $\beta_-\{\square_{c-s}\}$ ). On the other hand, without any  $\partial$ -saddle separatrix on the boundary, its COT symbol is simply written as  $\beta_\pm\{\lambda_\pm\}$ . In  $\square_{c\pm s}$ , we arrange the COT symbols for the internal structures in each quasi-essential  $\partial$ -saddle separatrix in a counter-clockwise circular order as follows.

$$\square_{c\pm} = \{c_+, c_-\}, \quad \square_{c\pm s} := \square_{c\pm} \cdots \square_{c\pm} \quad (s > 0), \quad \square_{c\pm s} := \lambda_\pm \quad (s = 0).$$

**( $c_\pm$  structures)** There are one-dimensional orbit structures with a boundary attached with a quasi-inessential self-connected  $\partial$ -saddle separatrix as shown in Figure 17(b), whose COT symbols are given by  $c_\pm$ . We use the subscript + (resp. -) when the flow direction along the boundary is counter-clockwise (resp. clockwise). In the region enclosed by the  $\partial$ -saddle separatrix and the boundary, a periodic annulus  $\square_{b\pm}$  is necessarily contained, and any number of  $c_\pm$  orbit structures can be attached to the boundary. Hence, we can express the orbit structures as  $c_\pm(\square_{b\pm}, \square_{c\mp s})$ .

## A.2. Local orbit structures with essential saddle connections.

**A.2.1. Shorthand notations in COT symbols.** According to Lemma 3.4, there are two local orbit structures with essential saddle connections, which are either simply essential or fully essential. When there is a boundary in the flow domain, local orbit structures of structurally Hamiltonian flows can be complex. Some shorthand notations are required to express these structures with COT symbols. For any  $k \in \mathbb{Z}_{>0}$ , we introduce the following shorthand notations.

$$\begin{aligned} \square_{C_+} &:= (\square_{b-}, \square_{cs+}, \square_{cs+}) = (\square_{b-}, \square_{cs+}^2), \\ \square_{C_-} &:= (\square_{b+}, \square_{cs-}, \square_{cs-}) = (\square_{b+}, \square_{cs-}^2), \\ \square_{C_{+-}} &:= ((\square_{b-}, \square_{cs+}^2), (\square_{b+}, \square_{cs-}^2)) = (\square_{C_+}, \square_{C_-}), \\ \square_{C_{-+}} &:= ((\square_{b+}, \square_{cs-}^2), (\square_{b-}, \square_{cs+}^2)) = (\square_{C_-}, \square_{C_+}), \\ (\square_{C_{+-}})^{k+1/2} &:= ((\square_{C_{+-}})^k, \square_{C_+}), \quad (\square_{C_{-+}})^{k+1/2} := ((\square_{C_{-+}})^k, \square_{C_-}), \\ \square_{\dot{C}_-} &:= (\square_{\dot{+}}, \square_{cs-}), \quad \square_{\dot{C}_+} := (\square_{\dot{-}}, \square_{cs+}). \end{aligned}$$

In each  $\square$ , the following can be substituted.

$$\begin{aligned} \square_{\dot{+}} &\in \{a_{\pm\dot{+}}, \alpha_{+\dot{-}}, \beta_{2+4k\dot{+}}, \beta_{4+4k\dot{+}}, \lambda_{\dot{+}}\}, \quad \square_{\dot{-}} \in \{a_{\pm\dot{-}}, a_{-\dot{+}}, \beta_{2+4k\dot{-}}, \beta_{4+4k\dot{-}}, \lambda_{\dot{-}}\}, \\ \square_{b+} &\in \{b_{+\pm}, \beta_+, \beta_{2+4k\dot{-}\dot{+}}, \beta_{4+2(k_1+k_2)+\dot{+}\dot{+}}, \beta_{4+2(k_1+k_2)+\dot{-}\dot{-}}, \beta_{4+2(k+k)+\dot{-}\dot{+}}, \\ &\quad \beta_{8+2(k_1+k_2)+\dot{+}\dot{+}}, \beta_{4+2(k_1+k_2)+\dot{-}\dot{-}}, \sigma_+\}, \\ \square_{b-} &\in \{b_{-\pm}, \beta_-, \beta_{2+4k\dot{+}\dot{-}}, \beta_{4+2(k_1+k_2)-\dot{-}\dot{-}}, \beta_{4+2(k_1+k_2)-\dot{+}\dot{+}}, \beta_{4+2(k+k)-\dot{+}\dot{+}}, \\ &\quad \beta_{8+2(k_1+k_2)-\dot{-}\dot{-}}, \beta_{4+2(k_1+k_2)-\dot{+}\dot{+}}, \sigma_-\}. \end{aligned}$$

A.2.2. *Orbit structures with singly essential saddle connections.* Let us refer to a separatrix not parallel to the boundary as a *non-boundary-parallel separatrix*. In other words, a non-boundary-parallel separatrix is a separatrix that cannot be continuously transformed in the torus into a separatrix on the boundary while keeping the endpoints on the boundary fixed. The orientation of the separatrices depends on whether the number of non-boundary-parallel separatrices is odd or even. See Figure 18(a). When the number of non-boundary-parallel separatrices on the boundary is odd, the outermost saddle separatrices on the boundary have the same direction. On the other hand, when the number is even, the directions are opposite. The COT symbol of this structure needs to be different depending on the current position and whether the number of non-boundary-parallel separatrices are odd or even. Furthermore, since quasi-essential saddle separatrices can be attached to the boundary, we express their number in the COT symbol.

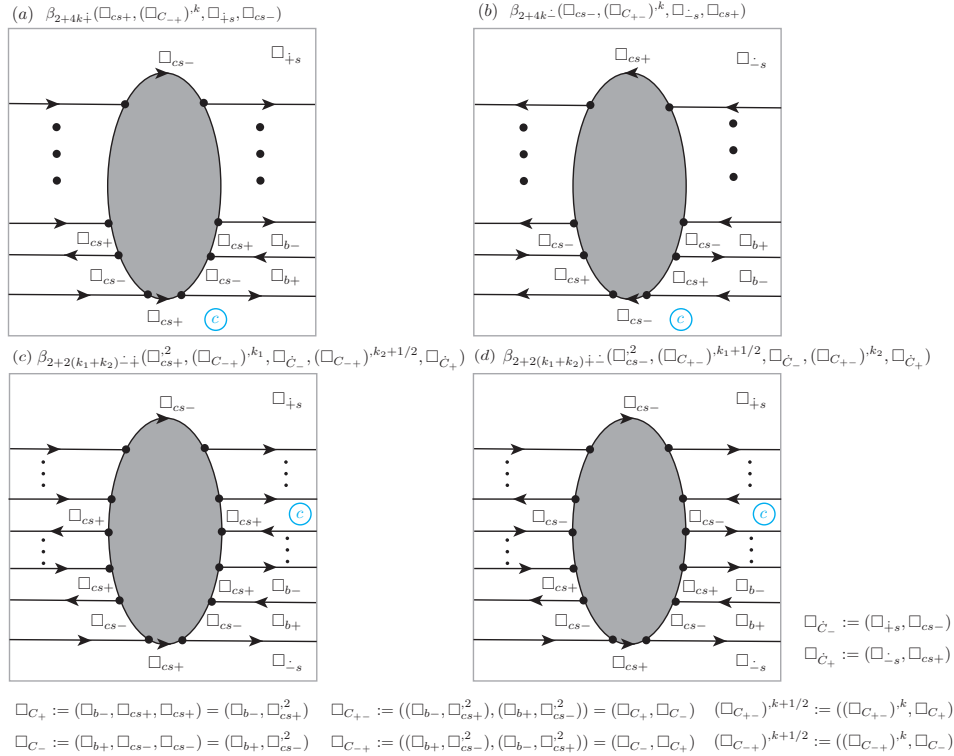


FIGURE 18. List of singly essential saddle connections on the boundary with an odd number of non-boundary-parallel separatrices.

( $\beta_{2+4k\pm}$ ,  $\beta_{2+2(k_1+k_2)\pm}$  **structures**) When there is an odd number of quasi-essential non-boundary-parallel separatrices, four local orbit structures appear as shown in Figure 18. This one-dimensional structure has non-boundary-parallel separatrices connecting the  $1 + 2k$  boundary separatrices and  $4k + 2$   $\partial$ -saddles on the boundary. See Figure 18. Since the saddle connections divide the annular region into  $1 + 2k$  regions, the COT symbol is defined according to the combination of

heights of the Hamiltonian functions in these regions. Accordingly, the orbit structures can be classified into four types as shown in Figure 18.

- Suppose that the current is essential. If the value of the Hamiltonian function in the one-dimensional structure is higher (resp. lower) than that at the current, the COT symbol for this structure is given by  $\beta_{2+4k\dot{+}}$  (resp.  $\beta_{2+4k\dot{-}}$ ) as in Figure 18(a) (resp. Figure 18(b)).
- Suppose that the current is inessential. If the value of the Hamiltonian function in the one-dimensional structure is higher (resp. lower) than that at the current, the COT symbol for this structure is given by  $\beta_{2+2(k_1+k_2)\dot{+}\dot{-}}$  (resp.  $\beta_{2+2(k_1+k_2)\dot{-}\dot{+}}$ ) as in Figure 18(c) (resp. Figure 18(d)).

Using Figure 18, we specify the COT symbols for the internal orbit structures as follows:

- Figure 18(a)  $\beta_{2+4k\dot{+}}(\square_{cs+}, (\square_{C-+})^k, \square_{\dot{C}+})$ .
- Figure 18(b)  $\beta_{2+4k\dot{-}}(\square_{cs-}, (\square_{C+-})^k, \square_{\dot{C}-})$ .
- Figure 18(c)  $\beta_{2+2(k_1+k_2)\dot{-}\dot{+}}(\square_{cs+}^2, (\square_{C-+})^{k_1}, \square_{\dot{C}-}, (\square_{C-+})^{k_2+1/2}, \square_{\dot{C}+})$ .
- Figure 18(d)  $\beta_{2+2(k_1+k_2)\dot{+}\dot{-}}(\square_{cs-}^2, (\square_{C+-})^{k_1+1/2}, \square_{\dot{C}-}, (\square_{C+-})^{k_2}, \square_{\dot{C}+})$ .

( $\beta_{4+4k\dot{\pm}}$ ,  $\beta_{4+4k\dot{\pm}}$ ,  $\beta_{4+2(k_1+k_2)\dot{\pm}\dot{\pm}}$ ,  $\beta_{4+2(k_1+k_2)\dot{\mp}\dot{-}}$  **structures**) When the number of non-boundary-parallel separatrices of a singly essential saddle connection  $C$  intersecting  $\partial S$  is even, we have the six local orbit structures shown in Figure 19. These one-dimensional structures have non-boundary-parallel separatrices connecting the  $2 + 2k$  boundary separatrices and  $4 + 4k$   $\partial$ -saddles. See Figure 19. Since the annular region is divided into  $2 + 2k$  regions by these saddle connections, the COT symbols must be assigned according to the height of the divided regions. As a result, we obtain the structure shown in Figure 19.

- Suppose that the current is essential. When the value of the Hamiltonian function of the one-dimensional structures is higher (resp. lower) than that at the current, we have the orbit structure of Figure 19(a) (resp. Figure 19(b)) and its COT symbol is given by  $\beta_{4+4k\dot{+}}$  (resp.  $\beta_{4+4k\dot{-}}$ ).
- Suppose that the current is inessential. When the value of the Hamiltonian function of the one-dimensional structure is higher than that at the current, and the values of the essential annuli adjacent to saddle connections and the current are equal, we have the orbit structure of Figure 19(c) and its COT symbol is given by  $\beta_{4+2(k_1+k_2)\dot{+}\dot{-}}$ .
- Suppose that the current is inessential. When the value of the Hamiltonian function of the one-dimensional structure is lower than that at the current, and the values of the essential annuli adjacent to saddle connections and the current are equal, we have the orbit structure of Figure 19(d) and its COT symbol is given by  $\beta_{4+2(k_1+k_2)\dot{-}\dot{+}}$ .
- Suppose that the current is inessential. When the value of the Hamiltonian function of the one-dimensional structure is lower than that at the current, and the value of the essential annuli adjacent to saddle connections is lower than that at the current, we have the orbit structure of Figure 19(e) and its COT symbol is given by  $\beta_{4+2(k_1+k_2)\dot{-}\dot{-}}$ .
- Suppose that the current is inessential. When the value of the Hamiltonian function of the one-dimensional structure is higher than that at the current, and the value of the essential annuli adjacent to saddle connections is lower

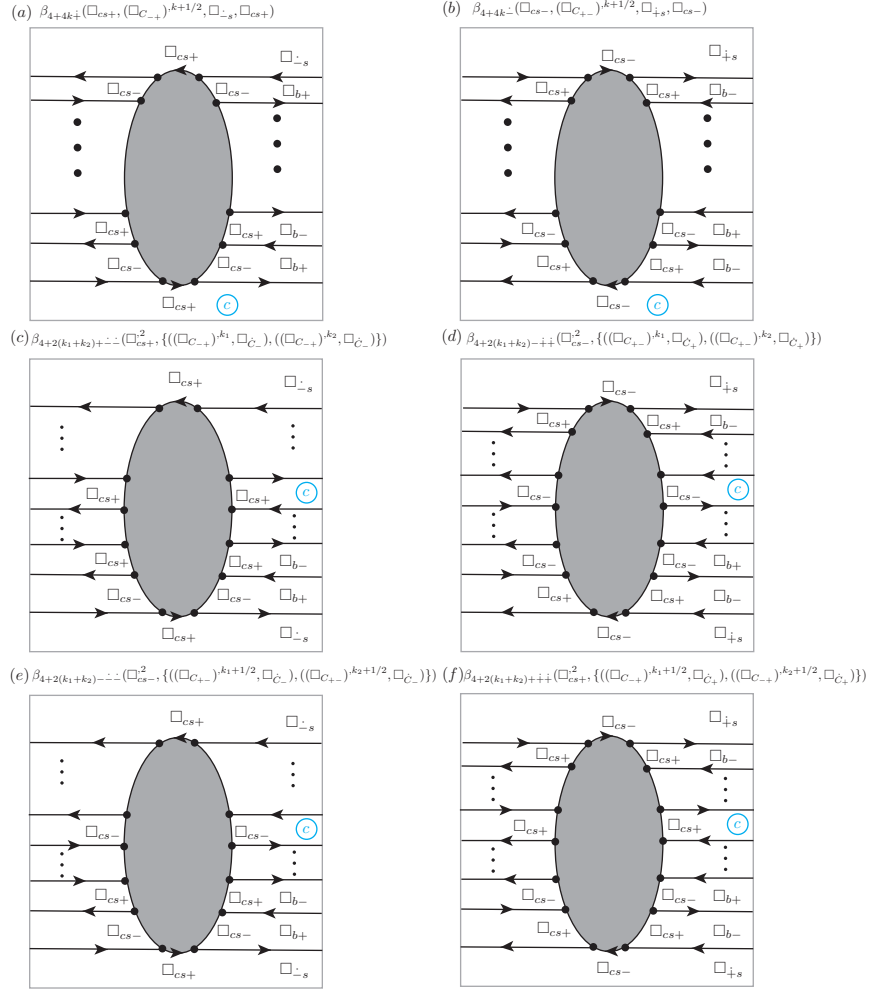


FIGURE 19. List of singly essential saddle connections on the boundary with an even number of non-boundary-parallel separatrices.

than that at the current, we have the orbit structure of Figure 19(f) and its COT symbol is given by  $\beta_{4+2(k_1+k_2)\dot{+}\dot{+}}$ .

Using Figure 19, we specify the COT symbols for the internal orbit structures as follows:

- Figure 19(a)  $\beta_{4+4k\dot{+}}(\square_{cs+}, (\square_{C_{-+}})^{k+1/2}, \square_{\dot{C}_+})$ ,
- Figure 19(b)  $\beta_{4+4k\dot{-}}(\square_{cs-}, (\square_{C_{+-}})^{k+1/2}, \square_{\dot{C}_-})$ ,
- Figure 19(c)  $\beta_{4+2(k_1+k_2)\dot{-}\dot{-}}(\square_{cs+}^2, \{((\square_{C_{-+}})^{k_1}, \square_{\dot{C}_-}), ((\square_{C_{-+}})^{k_2}, \square_{\dot{C}_-})\})$ ,
- Figure 19(d)  $\beta_{4+2(k_1+k_2)\dot{-}\dot{+}}(\square_{cs-}^2, \{((\square_{C_{+-}})^{k_1}, \square_{\dot{C}_+}), ((\square_{C_{+-}})^{k_2}, \square_{\dot{C}_+})\})$ ,
- Figure 19(e)  $\beta_{4+2(k_1+k_2)\dot{-}\dot{-}}(\square_{cs-}^2, \{((\square_{C_{+-}})^{k_1+1/2}, \square_{\dot{C}_-}), ((\square_{C_{+-}})^{k_2+1/2}, \square_{\dot{C}_-})\})$ ,
- Figure 19(f)  $\beta_{4+2(k_1+k_2)\dot{+}\dot{+}}(\square_{cs+}^2, \{((\square_{C_{-+}})^{k_1+1/2}, \square_{\dot{C}_+}), ((\square_{C_{-+}})^{k_2+1/2}, \square_{\dot{C}_+})\})$ ,

in which  $4k = 2k_1 + 2k_2$ . Note that we can choose an essential periodic orbit even if these structures are contained. Hence, we can construct a conversion algorithm for this case in a similar manner.

**A.2.3. Local orbit structures with a fully essential saddle connection.** Lemma 3.4 shows that there exists at most one boundary with fully essential saddle connections. Depending on the location of the current and the flow direction, we need to consider six local orbit structures as shown in Figure 20.

( $\beta_{8+2(k_1+k_2)\pm}$ ,  $\beta_{8+2(k_{1,1}+k_{1,2}+k_2)\pm\pm}$ ,  $\beta_{12+2(k_{1,1}+k_{1,2}+k_2)\pm\mp}$  **structures**) Since the fully essential saddle connection divides the torus  $S$  with boundary into  $8 + 2(k_1 + k_2)$ ,  $8 + 2(k_{1,1} + k_{1,2} + k_2)$ , or  $12 + 2(k_{1,1} + k_{1,2} + k_2)$  regions, it is necessary to assign COT symbols according to the heights of the Hamiltonian functions of the divided regions. As a result, we obtain the following six local orbit structures with different COT symbols as shown in Figure 20.

- Suppose that the current is essential. When the value of the Hamiltonian function of the one-dimensional structure is higher (resp. lower) than that at the current, we have the orbit structure of Figure 20(a) (resp. Figure 20(b)), and its COT symbol is given by  $\beta_{8+2(k_1+k_2)+}$  (resp.  $\beta_{8+2(k_1+k_2)-}$ ).
- Suppose that the current is inessential. When the value of the Hamiltonian function of the one-dimensional structure is lower than that at the current, and the value of the essential annuli adjacent to the saddle connection is lower than that at the current, we have the orbit structure of Figure 20(c), and its COT symbol is given by  $\beta_{8+2(k_{1,1}+k_{1,2}+k_2)--}$ .
- Suppose that the current is inessential. When the value of the Hamiltonian function of the one-dimensional structure is higher than that at the current, and the value of the essential annuli adjacent to the saddle connections is higher than that at the current, we have the orbit structure of Figure 20(d), and its COT symbol is given by  $\beta_{8+2(k_{1,1}+k_{1,2}+k_2)++}$ .
- Suppose that the current is inessential. When the value of the Hamiltonian function of the one-dimensional structure is higher than that at the current, and the value of the essential annuli adjacent to the saddle connections equals that at the current, we have the orbit structure of Figure 20(e), and its COT symbol is given by  $\beta_{12+2(k_{1,1}+k_{1,2}+k_2)-+}$ .
- Suppose that the current is inessential. When the value of the Hamiltonian function of the one-dimensional structure is lower than that at the current, and the value of the essential annuli adjacent to the saddle connections equals that at the current, we have the orbit structure of Figure 20(f), and its COT symbol is given by  $\beta_{12+2(k_{1,1}+k_{1,2}+k_2)+-}$ .

Using Figure 20, we specify the COT symbols for the internal orbit structures as follows:

- Figure 20(a)  $\beta_{8+2(k_1+k_2)+}(\square_{cs+}^4, \{(\square_{C-+})^{k_1+1/2}, (\square_{C-+})^{k_2+1/2}\})$ ,
- Figure 20(b)  $\beta_{8+2(k_1+k_2)-}(\square_{cs-}^4, \{(\square_{C+-})^{k_1+1/2}, (\square_{C+-})^{k_2+1/2}\})$ ,
- Figure 20(c)  $\beta_{8+2(k_{1,1}+k_{1,2}+k_2)--}((\square_{cs-}^2, \{(\square_{C+-})^{k_{1,1}}, (\square_{C+-})^{k_{1,2}}\}, \square_{cs-}^4, \square_{b-}, (\square_{C+-})^{k_2+1/2})$ ,
- Figure 20(d)  $\beta_{8+2(k_{1,1}+k_{1,2}+k_2)++}((\square_{cs+}^2, \{(\square_{C-+})^{k_{1,1}}, (\square_{C-+})^{k_{1,2}}\}, \square_{cs+}^4, \square_{b+}, (\square_{C-+})^{k_2+1/2})$ ,



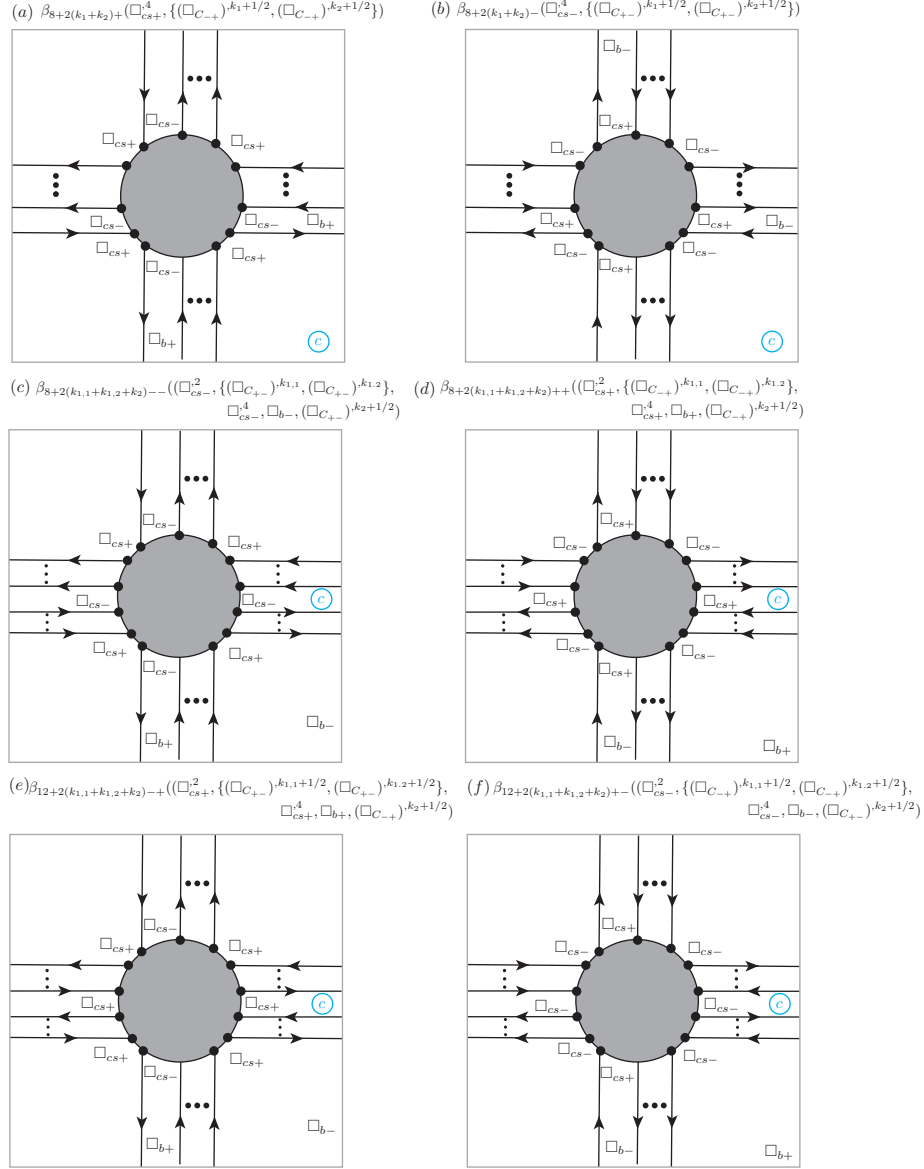


FIGURE 20. List of singly essential saddle connections on the boundary with an even number of non-boundary-parallel separatrices.

- Figure 20(e)  $\beta_{12+2(k_{1,1}+k_{1,2}+k_2)-}((\square_{c_s+}^2, \{(\square_{C_{+-}})^{k_{1,1}+1/2}, (\square_{C_{+-}})^{k_{1,2}+1/2}\}), \square_{c_s+}^4, \square_{b+}, (\square_{C_{+-}})^{k_2+1/2}),$
- Figure 20(f)  $\beta_{12+2(k_{1,1}+k_{1,2}+k_2)+}((\square_{c_s-}^2, \{(\square_{C_{+-}})^{k_{1,1}+1/2}, (\square_{C_{+-}})^{k_{1,2}+1/2}\}), \square_{c_s-}^4, \square_{b-}, (\square_{C_{+-}})^{k_2+1/2}),$

where  $k_1, k_2, k_{1,1}, k_{1,2} \geq 0$ . We remark that we have no essential periodic orbit if a fully essential saddle connection exists. Hence, we need to consider a different conversion algorithm in this case.

**Acknowledgements** The authors would like to thank Dr. Takeshi Matsumoto for providing the stream function data used in the present paper. We would also like to thank the members of Technology Research & Innovation, BIPROGY Inc. for useful discussions.

#### REFERENCES

- [1] Claude Basdevant and Thierry Philipovitch. On the validity of the “weiss criterion” in two-dimensional turbulence. *Physica D: Nonlinear Phenomena*, 73(1-2):17–30, May 1994. 1
- [2] Milton Cobo, Carlos Gutierrez, and Jaume Llibre. Flows without wandering points on compact connected surfaces. *Transactions of the American Mathematical Society*, 362(9):4569–4580, 2010. 3.2, 4.1
- [3] Marie Farge. Wavelet transforms and their applications to turbulence. *Annual Review of Fluid Mechanics*, 24(1):395–458, January 1992. 1
- [4] Gilbert Hector and Ulrich Hirsch. *Introduction to the Geometry of Foliations: Part B*. Springer, 1983. 2.1
- [5] B.L. Hua and P. Klein. An exact criterion for the stirring properties of nearly two-dimensional turbulence. *Physica D: Nonlinear Phenomena*, 113(1):98–110, February 1998. 1
- [6] Andres Koropec and Fabio Armando Tal. Strictly toral dynamics. *Inventiones mathematicae*, 196(2):339–381, 2014. 2.2
- [7] Tian Ma and Shouhong Wang. *Geometric theory of incompressible flows with applications to fluid dynamics*. Number 119. American Mathematical Soc., 2005. 1, 3.1
- [8] James C. McWilliams. The vortices of two-dimensional turbulence. *Journal of Fluid Mechanics*, 219(1):361, October 1990. 1
- [9] T Sakaajo and T Yokoyama. Tree representation of topological streamline patterns of structurally stable 2d hamiltonian vector fields in multiply conected domains. *The IMA Journal of Applied Mathematics*, 83:380–411, 2018. 1
- [10] Takashi Sakaajo and Keiichi Itatani. Topological identification of vortical flow structures in the left ventricle of the heart. *SIAM Journal on Imaging Sciences*, 16(3):1491–1519, August 2023. 1
- [11] Takashi Sakaajo and Tomoo Yokoyama. Discrete representations of orbit structures of flows for topological data analysis. *Discrete Mathematics, Algorithms and Applications*, 15(06), September 2022. 1
- [12] P Tabeling. Two-dimensional turbulence: a physicist approach. *Phys. Rep.*, 362(1):1–62, May 2002. 1
- [13] Tomoki UDA, Takashi SAKAJO, Masaru INATSU, and Kazuki KOGA. Identification of atmospheric blocking with morphological type by topological flow data analysis. *Journal of the Meteorological Society of Japan. Ser. II*, 99(5):1169–1183, 2021. 1
- [14] Tomoki Uda, Tomoo Yokoyama, and Takashi Sakaajo. Algorithms converting streamline topologies for 2d hamiltonian vector fields using reeb graphs and persistent homology. *Transactions of the Japan Society for Industrial and Applied Mathematics*, 29(2):187–224, 2019. 1, 4.5, 4.5.1, 6
- [15] TETSUO Yokoyama and TOMOO Yokoyama. COT representations of 2D hamiltonian flows and their computable applications. *preprint*, 2021. 1, 4.5.3
- [16] Tomoo Yokoyama and Takashi Sakaajo. Word representation of streamline topologies for structurally stable vortex flows in multiply connected domains. *Proceedings of the Royal Society A: Mathematical, Physical and Engineering Sciences*, 469(2150):20120558, 2013. 1, 4.5.3

DEPARTMENT OF MATHEMATICS, OSAKA DENTAL UNIVERSITY, HIRAKATA, 573-1121 JAPAN  
*Email address:* `kimura-m@cc.osaka-dent.ac.jp`

DEPARTMENT OF MATHEMATICS, KYOTO UNIVERSITY, KYOTO, 606-8502 JAPAN  
*Email address:* `sakajo@math.kyoto-u.ac.jp`

DEPARTMENT OF MATHEMATICS, SAITAMA UNIVERSITY, SAITAMA, 338-8570 JAPAN  
*Email address:* `tyokoyama@rimath.saitama-u.ac.jp`